Temporal variability and driving factors of the carbonate system in the Aransas Ship Channel, TX, USA: A time-series study

Melissa R. McCutcheon[1], Hongming Yao[1,#], Cory J. Staryk[1], Xinping Hu[1]

[1] Harte Research Institute for Gulf of Mexico Studies, Texas A&M University – Corpus Christi, TX 78412, USA
[#] current address: Shenzhen Engineering Laboratory of Ocean Environmental Big Data Analysis and Application, Shenzhen Institute of Advanced Technology, Chinese Academy of Sciences, Shenzhen 518055, China

---

Correspondence to: Melissa R. McCutcheon (melissa.mccutcheon@tamucc.edu)

Keywords: $p\mathrm{CO_2}$, acidification, diel variability, seasonal variability, autonomous sensors

Abstract

~~Estuaries~~ is affected by an array of co-occurring biogeochemical and anthropogenic processes, resulting in substantial heterogeneity in water chemistry, including carbonate chemistry parameters such as pH and partial pressure of CO_2 (pCO_2).~~The coastal ocean experiencesare complex systems with substantial heterogeneity in water chemistry, including carbonate chemistry parameters such as pH and partial pressure of CO_2 (pCO_2),~~

~~because of the diversity of co-occurring biogeochemical processes~~. To better understand ~~estuarine~~ coastal and estuarine acidification and air-sea CO_2 fluxes ~~from estuaries~~, it is important to study baseline variability and driving factors of carbonate chemistry. Using both discrete bottle sample collection (2014-2020) and hourly sensor measurements (2016-2017), we explored temporal variability, from diel to interannual scales, in the carbonate system (specifically pH and pCO_2) at the Aransas Ship Channel located in northwestern Gulf of Mexico. Using other co-located environmental sensors, we also explored the driving factors of that variability. Both sampling methods demonstrated significant seasonal variability at the location, with highest pH (lowest pCO_2) in the winter and lowest pH (highest pCO_2) in the summer. Significant diel variability was also evident from sensor data, but the time of day with elevated pCO_2/depressed pH was not consistent across the entire monitoring period, sometimes reversing from what would be expected from a biological signal. Though seasonal and diel fluctuations were smaller than many other areas previously studied, carbonate chemistry parameters were among the most important environmental parameters to distinguish between time of day and between seasons. It is evident that temperature,

Formatted: Indent: First line: 0.5"

biological activity, freshwater inflow, and tide level (despite the small tidal range) are all important controls on the system, with different controls dominating at different time scales. The results suggest that the controlling factors of the carbonate system may not be exerted equally on both pH and pCO_2 on diel timescales, causing separation of their diel or tidal relationships during certain seasons. Despite known temporal variability on shorter timescales, discrete sampling was generally representative of the average carbonate system and average air-sea CO_2 flux on a seasonal and annual basis ~~based on comparison~~when compared with sensor data.

1. Introduction

Coastal waters, especially e~~E~~stuaries, experience substantial spatial and temporal heterogeneity in water chemistry—including carbonate chemistry parameters such as pH and partial pressure of CO_2 (pCO_2)—due to the diversity of co-occurring biogeochemical and anthropogenic processes ~~the dynamic environments where the coast and freshwater inflows meet the ocean, and coastal waters are economically and ecologically important because they are biological hotspots, but they are also heavily influenced by anthropogenic activity. Because of the diversity of co-occurring biogeochemical processes, estuaries experience substantial spatial and temporal heterogeneity in water quality and chemistry, including carbonate chemistry parameters such as pH and partial pressure of CO_2 (pCO_2)~~ (Hofmann et al., 2011; Waldbusser and Salisbury, 2014). Carbonate chemistry~~, or the speciation of inorganic carbon in seawater,~~ is important ~~for two main reasons. First,~~because an addition of CO_2 acidifies seawater,~~ whether it is a result of uptake from the atmosphere (generally acknowledged as ocean acidification, or OA) or it is produced by biogeochemical processes in the water (that may intensify or~~

~~alleviate the effects of OA). This is problematic because a~~~~A~~ and acidification can negatively affect marine organisms~~, especially those that construct calcium carbonate shells and skeletons~~ (Barton et al., 2015; Bednaršek et al., 2012; Ekstrom et al., 2015; Gazeau et al., 2007; Gobler and Talmage, 2014). ~~Second, the ocean contributes substantially to the global carbon budget, which is important to understand because of climate change implications. Despite~~ Additionally, despite the small surface area of coastal waters relative to the global ocean, coastal waters are recognized as important contributors in global carbon cycling (Borges, 2005; Cai, 2011; Laruelle et al., 2018).

While ~~open ocean environments are relatively well studied and understood regarding~~ carbonate chemistry, acidification, and air-sea CO_2 fluxes are relatively well studied and understood in open ocean environments,~~,~~ large uncertainties remain in ~~estuarine~~ coastal environments. Estuaries are especially challenging to fully understand because of the heterogeneity between and within estuaries that is driven by diverse processes operating on different time scales such as river discharge, nutrient and organic matter loading, stratification, and coastal upwelling (Jiang et al., 2013; Mathis et al., 2012). The traditional sampling method for carbonate system characterization involving discrete water sample collection and laboratory analysis is known to lead to biases in average pCO_2 and CO_2 flux calculations due to daytime sampling that neglects to capture diel variability (Li et al., 2018). Mean diel ranges in pH can exceed 0.1 unit in many coastal environments, ~~and single day ranges can exceed 1 pH unit, with~~ and especially high diel ~~variability~~ranges (even exceeding 1 pH unit) have been reported in biologically productive areas or areas with higher mean pCO_2 (Challener et al., ~~2015~~2016; Cyronak et al., 2018; Schulz and Riebesell, 2013; Semesi et al., 2009; Yates et al., 2007). These diel ranges can far surpass the magnitude of the changes in open ocean surface waters that have occurred since the start of the industrial revolution and rival spatial variability in productive systems, indicating their importance for a full understanding of the carbonate system.

Despite the need for high-frequency measurements, sensor deployments have been limited in estuarine environments (especially compared to their extensive use in the open ocean) because of the challenges associated with varying conditions, biofouling, and sensor drift (Sastri et al., 2019). Carbonate chemistry monitoring in the Gulf of Mexico (GOM)~~, and especially its estuaries~~, has been relatively minimal compared to the United States east and west coasts. The GOM estuaries~~, where this study takes place,~~ currently have less exposure to concerning levels of acidification than other estuaries because of their high temperatures (causing water to hold less CO_2 and support high productivity year-round) and often suitable river chemistries (i.e.~~,~~ relatively high buffer capacity) (McCutcheon et al., 2019; Yao et al., 2020). However, respiration-induced acidification is present in both the open GOM (e. g., subsurface water influenced by the Mississippi River Plume and outer shelf region near the Flower Garden Banks National Marine Sanctuary) and GOM estuaries, and most estuaries in the northwestern GOM have also experienced long-term acidification (Cai et al., 2011; Hu et al., ~~2018~~2015, ~~2015~~2018; Kealoha et al., 2020; McCutcheon et al., 2019; Robbins and Lisle, 2018). This known acidification as well as the relatively high CO_2 ~~fluxes~~ efflux from the estuaries of the northwest GOM ~~(which may change our understanding of global estuarine contribution to the carbon budget)~~ illustrates the necessity to study the baseline variability and driving factors of carbonate chemistry in the region. In this study, we explored temporal variability in the carbonate system in Aransas Ship Channel—a tidal inlet where the lagoonal estuaries meet the coastal waters in a semi-arid region of the northwestern GOM—using both discrete bottle sample collection and hourly sensor measurements, and we explored the driving factors of that variability using data from other co-located environmental sensors.

2. Materials and Methods

2.1 Location

Autonomous sensor monitoring and discrete water sample collections for laboratory analysis of carbonate system parameters were performed in the Aransas Ship Channel (ASC, located at 27˚50'17"N, 97˚3'1"W). ~~The Aransas Ship Channel~~ASC is one of the few permanent tidal inlets that intersect a string of barrier islands and connect the GOM coastal waters with the lagoonal estuaries in the northwest GOM (Fig. 1). ~~The Aransas Ship Channel~~ASC provides the direct connection between the ~~nwGOM~~ northwestern GOM and the Mission-Aransas Estuary (Copano and Aransas Bays) to the north and Nueces Estuary (Nueces and Corpus Christi Bays) to the south (Fig. 1). The region is microtidal,- with a small tidal range relative to many other estuaries, ranging from ~ 0.6 m tides on the open coast to less than 0.3 m in upper estuaries~~with a relatively small tidal range, ranging from The tidal range in the region is small, with around~~ ~~~ 0.6 m tides on the open coast and~~ to ~~less than 0.3 m in the~~ upper ~~estuaries~~ (Montagna et al., 2011). Mission-Aransas Estuary (MAE) is fed by two small rivers, the Mission (1787 km^2 drainage basin) and Aransas (640 km^2 drainage basin) Rivers (http://waterdata.usgs.gov/), which both experience low base flows punctuated by periodic high flows during storm events. MAE has an average residence time of one year

(Solis and Powell, 1999), so there is a substantial lag between time of rainfall and riverine delivery to ~~the Aransas Ship Channel~~ASC in the lower estuary. A significant portion of riverine water flowing into Aransas Bay originates from the larger rivers further northeast on the Texas coast via the Intracoastal Waterway (i.e., Guadalupe River (26,625 km^2 drainage basin) feeds San Antonio Bay and has a much shorter residence time of nearly 50 days) (Solis and Powell, 1999; USGS, 2001).

~~**Fig 1.** Location of Aransas Ship Channel where this study took place (arrow) and surrounding bay systems.~~

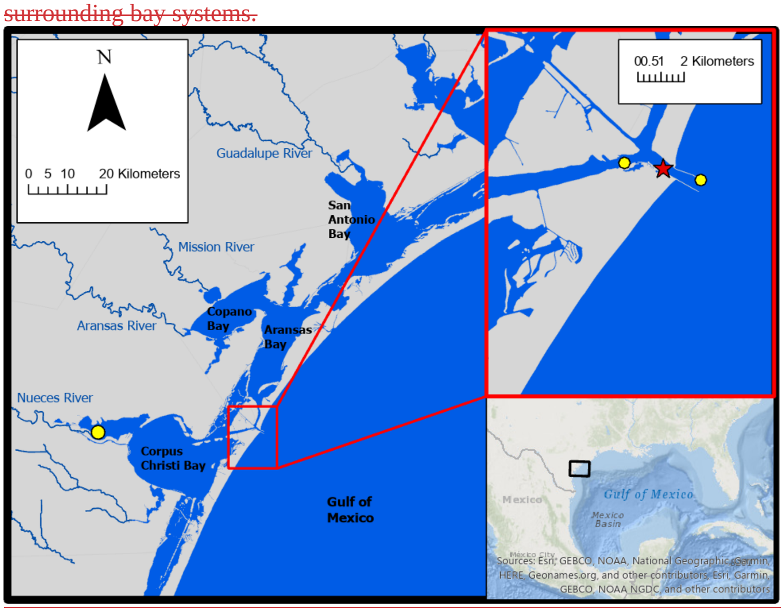

Fig 1. Study area. The location of monitoring in the Aransas Ship Channel (red star) and the ~~is denoted with a red star. The~~ locations of NOAA stations used for wind data (yellow circles) are ~~denoted with yellow circle~~shown.

Formatted: Font: Not Bold

Formatted: Normal, Line spacing: single

2.2 Continuous Monitoring

Autonomous sensor monitoring (referred to throughout as continuous monitoring) of pH and pCO_2 was conducted from Nov. 8, 2016 to Aug. 23, 2017 at the University of Texas Marine Science Institute's research pier in ~~the Aransas Ship Channel~~ASC~~. The sensor deployment was shorter than intended because the pier where the sensors were deployed was destroyed in the aftermath of Hurricane Harvey in 2017~~. ~~The~~ Hourly pH data were collected using an SAtlantic® SeaFET pH sensor (on total pH scale) and hourly pCO_2 data were collected using a Sunburst® SAMI-CO_2. ~~Temperature~~ Hourly temperature and salinity data were measured by a YSI® 600OMS V2 sonde. ~~Hourly~~ All hourly data were ~~(~~ single ~~hourly~~ measurements~~,~~ ~~measured~~taken on the hour.~~)~~ The average difference between sensor pH and discrete quality assurance samples measured spectrophotometrically in the lab was used to establish a correction (-0.05) based on a single calibration point across the entire sensor pH dataset (Bresnahan et al., 2014). See supplemental materials for additional sensor deployment and quality assurance

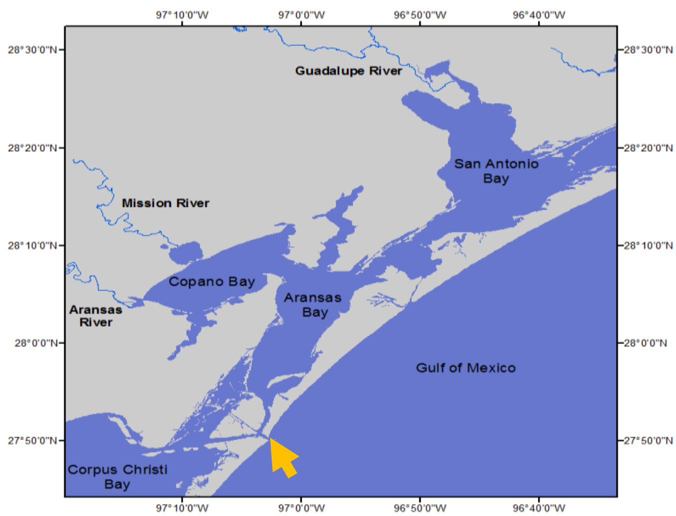

information.collected by all sensors (pH, *p*CO_2, salinity, and temperature) were saved in the onboard data loggers and downloaded during service trips to the field site. Sensor failures or pump failures occurred for short periods of time throughout the deployment. Measurements were recorded on 262 individual days, with 176 of those days having the full set of 24 (hourly) measurements.

Ideally, *in-situ* sensors should be deployed under the sea surface. However, to reduce the maintenance cost and effort for sensors deployed in warm water that experiences intense biofouling, the sensors were set up to measure pH and *p*CO_2 from an *ex situ* position using *in situ* seawater. Water was pumped from ~1 m below the sea surface into the bottom spigot of a 100-Qt cooler that housed the SAMI-CO2 and SeaFET sensors. To allow water outflow, a 1" hole was drilled at the opposite side of the spigot near the top of the cooler rim, allowing water to flow back to the sea surface. The pump was programmed to turn on 20 minutes before each hour, pumping more than enough water to fully flush the cooler, and sensors recorded measurements on the hour. The YSI sonde was deployed directly into the Aransas Ship ChannelASC inside a 2" PVC pipe at ~1 m below the sea surface.

Visits to the field site were conducted every two weeks to service all sensors and clean the cooler. Additionally, duplicate, discrete water samples were collected on the hour during service trips for quality assurance of sensor data and to check that surface water and cooler chemistries aligned. (See supplemental materials for additional information about discrete quality assurance samples, removal of suspicious sensor data, and a direct comparison of discrete quality assurance samples to sensor data). The same methods used for discrete sampling analysis apply for these samples (see section 2.3).

Samples were collected from the channel near the pump inlet and from the cooler that housed the sensors, and water temperature and salinity were measured using a handheld YSI data sonde. quality assuranceThe average difference between sensor pH and laboratory pH (from the cooler) was used to establish a correction of -0.05 to the final *in-situ* pH data since the SeaFET may experience drift. The average difference between sensor pH and laboratory pH (from the cooler) was used to establish a correction of -0.05 to the final *in-situ* pH data since the SeaFET may experience drift. The difference between the sensor pCO_2 and calculated pCO_2 is reported, but it is not used for a correction since the spectrophotometric measurements of the SAMI-CO2 should not experience drift. Sensor data were discarded from analysis during known periods of pump failure when cooler chemistry separated from that of the Aransas Ship Channel.

2.3 Discrete Sample Collection and Sample Analysis

In addition to the discrete sample collections that occurred for quality assurance during sensor servicing visits, longLong-term monitoring via discrete water sample collection was conducted at the Aransas Ship ChannelASC from May 2, 2014 to February 25, 2020 (in addition to the discrete, quality assurance sample collections). Sampling was conducted from a small vessel at a station very near to the sensor deployment every two weeks during the summer months and monthly during the winter months from a small vessel at a station near (<20 m from) the sensor deployment. Water sample collection followed standard protocol for ocean carbonate chemistry studies (Dickson et al., 2007). Ground glass borosilicate bottles (250 mL) were filled with surface water and preserved with 100 µL saturated mercury chloride ($HgCl_2$). Apiezon®

grease was applied to the bottle stopper, which was then secured to the bottle using a rubber band and a nylon hose clamp.

These samples were used for laboratory dissolved inorganic carbon (DIC) and pH measurements. DIC was measured by injecting 0.5 mL of sample into 1 ml 10% H_3PO_4 (balanced by 0.5 M NaCl) with a high-precision Kloehn syringe pump. The CO_2 gas produced through sample acidification was then stripped using high-purity nitrogen gas and carried into a Li-Cor infrared gas detector. DIC analyses had a precision of 0.1%. Certified Reference Material (CRM) was used to ensure the accuracy of the analysis (Dickson et al. 2003). For samples with salinity>20, pH was measured using a spectrophotometric method at 25 ± 0.1°C (Carter et al. 2003) and the Douglas and Byrne (2017) equation. Analytical precision of the spectrophotometric method for pH measurement was ±0.0004 pH units. A calibrated Orion Ross glass pH electrode was used to measure pH at 25 ± 0.1°C for samples with salinity<20, and analytical precision was ±0.01 pH units. All pH values obtained using the potentiometric method were converted to total scale at *in situ* temperature (Millero 2001). Salinity of the discrete samples was measured using a benchtop salinometer calibrated by MilliQ water and a known salinity CRM. For discrete samples, pCO_2 was calculated in CO2Sys for Excel using laboratory-measured salinity, DIC, pH, and *in situ* temperature for calculations. Carbonate speciation calculations were done using Millero (2010) carbonic acid dissociation constants (K_1 and K_2), Dickson (1990) bisulfate dissociation constant, and Uppström (1974) borate concentration.

2.4 Calculation of CO_2 fluxes

Formatted: Font: Italic

Formatted: Font: Italic

Formatted: Font: Italic, Subscript

Formatted: Font: Italic

Formatted: Indent: First line: 0"

2.4 Data Processing and Statistical Analyses

For the discrete samples, $p\mathrm{CO_2}$ was calculated using CO2Sys for Excel. Carbonate speciation calculations were done using Millero (2010) carbonic acid dissociation constants (K_1 and K_2), Dickson (1990) bisulfate dissociation constant, and Uppström (1974) borate concentration. Temporal variability was investigated in the form of seasonal and diel variability (Tables 1-2). For seasonal analysis, December to February was considered winter, March to May was considered spring, June to August was considered summer, and September to November was considered fall. Two-way ANOVAs were used to examine differences in parameter means between seasons, using differences between monitoring methods as the second factor (as differences between seasons may not be the same between monitoring methods, Table 3). Since there was a significant interaction in the two-way ANOVA, the differences between seasons were investigated within each monitoring method. Post-hoc multiple comparisons (between seasons within sampling types) were conducted using the Westfall adjustment (Westfall, 1997). For diel comparisons, daytime and nighttime variables were defined as 09:00-15:00 local standard time and 21:00-03:00 local standard time, respectively, based on the 6-hour periods with highest and lowest photosynthetically active radiation (PAR; data obtained from the Mission-Aransas National Estuarine Research Reserve (MANERR) at https://missionaransas.org/science/download-data. Paired *t*-tests, comparing the daytime mean with the nighttime mean on respective days, were used to look for significant differences between daytime and nighttime parameter values across the full sampling period and within each season (Table 2).

Equation 1 was used for air-water CO_2 flux calculations (Wanninkhof, 1992; Wanninkhof et al., 2009). Positive flux values indicate CO_2 emission from the water into the atmosphere (the estuary acting as a source of CO_2), and negative flux values indicate CO_2 uptake by the water (the estuary acting as a sink for CO_2).

$$F = k\, K_0\, (pCO_{2,w} - pCO_{2,a}) \quad (1)$$

where k is the gas transfer velocity (in m d^{-1}), K_0 (in mol l^{-1} atm^{-1}) is the solubility constant of CO_2 (Weiss, 1974), and $pCO_{2,w}$ and $pCO_{2,a}$ are the partial pressure of CO_2 (in µatm) in the water and air, respectively.

We used the wind speed parameterization for gas transfer velocity (*k*) from Jiang et al. (2008) converted from cm h^{-1} to m d^{-1}, which is thought to be the best estuarine parameterization at this time (Crosswell et al., 2017), as it is a composite of *k* over several estuaries. The calculation of *k* requires a windspeed at 10 m above the surface, so windspeeds measured at 3 m above the surface were converted using the power law wind profile (Hsu, 1994; Yao and Hu, 2017). To assess uncertainty, other parameterizations with direct applications to estuaries in the literature were also used to calculate CO_2 flux (Raymond and Cole 2001; Ho et al. 2006). We note that parameterization of *k* based on solely windspeed is flawed because several additional parameters can contribute to turbulence including turbidity, bottom-driven turbulence, water-side thermal convection, tidal currents, and fetch (Wanninkhof 1992, Abril et al., 2009, Ho et al., 2104, Andersson et al., 2017), however it is currently the best option for this system given the limited investigations of CO_2 flux and contributing factors in estuaries.

Hourly averaged windspeed data ~~used in~~for use in CO_2 flux calculations were retrieved from the NOAA-controlled Texas Coastal Ocean Observation Network

Formatted: Subscript

(TCOON; https://tidesandcurrents.noaa.gov/tcoon.html). The Windspeed data from the closest nearest TCOON station with windspeed data, (Port Aransas Station, – located was located directly in the Aransas Ship ChannelASC, (further ~< 12 km inshore than from our monitoring location) was usedprioritized when data were available. , however there were several long periods of missing dataDuring periods of missing windspeed data at the Port Aransas Station, . To fill in the data gaps, wind speed data from nearby TCOON's Aransas Pass Station (~< 12 km offshore from monitoring location) were next used, and for all subsequent gaps, data from nearby TCOON's Nueces Bay Station (~ 40 km away) were used (Fig. 1; additional discussion of flux calculation and windspeed data can be found in supplementary materials). . Prior to 2016-08-05, only the Nueces Bay station was recording, so early discrete monitoring flux calculations used the farthest station. About 55 days (<20% of observations) during the continuous monitoring period used data from Nueces Bay station, and after the continuous monitoring period (2017-08-23 – 2020-02-25) only about nine days of wind data had to be retrieved from the Nueces Bay station. For those days during the 5+ year monitoring period that data were available at both the Port Aransas Station and the Nueces Bay station, the Nueces Bay Station did have higher windspeeds by an average of ~2.33 m/s. Given this offset and the distance of this station (along with the many other factors that complicate the calculation of fluxes through windspeed parameterization), the actual values of CO_2 flux should not be taken at face value, but can still be useful in comparing methods and seasonal/diel patterns.

For flux calculations from continuous monitoring data, each hourly measurement of $p$$CO_2$ was paired with the corresponding TCOON's measured hourly windspeed at each time pointhourly averaged windspeed for was used in flux calculations. For flux

Formatted: Font: (Default) Times New Roman

Formatted: Font: Italic

Formatted: Subscript

calculations from biweekly discrete samplessample data, the $p$$CO_2$ calculated for each sampled day was paired with the corresponding daily averaged windspeed (calculated from averaged the retrieved hourly averaged windspeeds) for flux calculationsdaily windspeeds were calculated from TCOON's measured hourly windspeeds and used in flux calculations for the respective day.

Monthly mean atmospheric xCO_2 data (later converted to $p$$CO_2$) for flux calculations were obtained from NOAA's flask sampling network of the Global Monitoring Division of the Earth System Research Laboratory at the Key Biscayne (FL, USA) station., when available Global averages of atmospheric xCO_2 were used when Key Biscayne data were unavailable. Each $p$$CO_2$ observation (whether using continuous or discrete data) was paired with the corresponding monthly averaged xCO_2 for flux calculations. Additional information and justification are available in supplemental materials. (https://www.esrl.noaa.gov/gmd/dv/data/index.php?site=KEY&parameter_name=Carbon%2BDioxide). For 2019 and 2020, whenData from Key Biscayne were not available for the entire period of our discrete sample collection, so xCO2 data from Key Biscayne were unavailable, monthly global average values were used (ftp://aftp.cmdl.noaa.gov/products/trends/co2/co2_mm_mlo.txt) to fill in missing values (16 months from January 2019 – February 2020). We justified this substitution of global average values because the monthly means between Key Biscayne and global xCO_2 over the initial 56 months of our discrete sampling only differed by 1.2 ±µatm (i.e. 0.3% ± 0.4%). Each $p$$CO_2$ observation (whether using continuous or discrete data) was paired with the corresponding monthly averaged windspeed for flux calculations.

Formatted: Font: Italic

Formatted: Subscript

2.45 Data Processing and Statistical Analyses

For the discrete samples, *p*CO_2 was calculated using CO2Sys for Excel. Carbonate speciation calculations were done using Millero (2010) carbonic acid dissociation constants (K_1 and K_2), Dickson (1990) bisulfate dissociation constant, and Uppström (1974) borate concentration. Temporal variability was investigated in the form of seasonal and diel variability (Tables 1-2). For seasonal analysis, December to February was considered winter, March to May was considered spring, June to August was considered summer, and September to November was considered fall. Two-way ANOVAs were used to examine differences in parameter means between seasons, using differences between monitoring methods as the second factor (as differences between seasons may not be the same between monitoring methods, Table 3). Since there was a significant interaction in the two-way ANOVA, the differences between seasons were investigated within each monitoring method. Post-hoc multiple comparisons (between seasons within sampling types) were conducted using the Westfall adjustment (Westfall, 1997). For diel comparisons, daytime and nighttime variables were defined as 09:00-15:00 local standard time and 21:00-03:00 local standard time, respectively, based on the 6-hour periods with highest and lowest photosynthetically active radiation (PAR; data obtained from the Mission-Aransas National Estuarine Research Reserve (MANERR) at https://missionaransas.org/science/download-data. Paired *t*-tests, comparing the daytime mean with the nighttime mean on respective days, were used to look for significant differences between daytime and nighttime parameter values across the full sampling period and within each season (Table 2).

2.65 Additional data retrieval and data processing Factors controlling the carbonate system parameters to investigate carbonate system variability and controls

All reported annual mean values are seasonally weighted to account for disproportional sampling between seasons. However, reported annual standard deviation is associated with the un-weighted, arithmetic mean (Table S1). Temporal variability was investigated in the form of seasonal and diel variability (Tables S1, S2, S3). For seasonal analysis, December to February was considered winter, March to May was considered spring, June to August was considered summer, and September to November was considered fall. It is important to note that the Fall season had much fewer continuous sensor observations than other seasons because of the timing of sensor deployment. For diel comparisons, daytime and nighttime variables were defined as 09:00-15:00 local standard time and 21:00-03:00 local standard time, respectively, based on the 6-hour periods with highest and lowest photosynthetically active radiation (PAR; data from co-located sensor, obtained from the Mission-Aransas National Estuarine Research Reserve (MANERR) at https://missionaransas.org/science/download-data). Diel ranges in parameters were calculated (daily maximum minus daily minimum) and only reported for days with the full 24 hours of hourly measurements (176 out of 262 measured days) to ensure that data gaps did not influence the diel ranges (Table S3).

Thermal versus non-thermal cControls on pCO_2 from thermal and non-thermal (i.e., combination of physical and biological) processes) were investigated following Takahashi et al. ((Takahashi et al., 2002)2002) over annual, seasonal, and daily time scales using both continuous and discrete data. (Table 4). Over any given time period,

Formatted: Font: (Default) Times New Roman

Formatted

Formatted: Font: Not Italic

Formatted: Indent: First line: 0.5"

this method uses the ratio of the ranges of temperature-normalized pCO_2 (pCO_2; ($pCO_{2,}$ non-thermalnt, Eq. 2) and the mean annual pCO_2 perturbed by the difference between mean and observed temperature (pCO_{2}-, tthermal, Eq. 3) to calculate the relative influence of non-thermal and thermal effects on pCO_2 (T/B, Eq. 4). When calculating annual T/B values with discrete data, only complete years (sampling from January to December) were included (2014 and 2020 were omitted). When calculating daily T/B values with continuous data, only complete days (24 hourly measurements) were included. The summary of annual T/B values from discrete data includes only 2015-2019 (n=5 years; 2014 and 2020 were omitted since monitoring did not occur throughout the entire year). Daily values from continuous data were only reported for those days with all 24 measurements.

$$pCO_{2,nonthermalt} = pCO_{2,obs} \times \exp[\,\delta \times (T_{mean} - T_{obs})] \qquad (32)$$

$$pCO_{2,thermal} = pCO_{2,mean} \times \exp[\,\delta \times (T_{obs} - T_{mean})] \qquad (23)$$

$$pCO_{2,nonthermal} = pCO_{2,obs} \times \exp[\,\delta \times (T_{mean} - T_{obs})] \qquad (3)$$

wWhere the value for δ (0.0411 °C^{-1}), which represents average [∂ *ln* pCO_2 / ∂ Temperature] from field observations, was taken directly from Yao and Hu (2017), T_{obs} is the observed temperature, and T_{mean} is the mean temperature over the investigated time period.

$$T/B = \frac{\max(pCO_{2,thermal}) - \min(pCO_{2,thermal})}{\max(pCO_{2,non-thermal}) - \min(pCO_{2,non-thermal})} \qquad (4)$$

Where a T/B greater than one indicates that temperature's control on pCO_2 is greater than the control from non-thermal factors (i.e. physical and biological processes) and a T/B less than one indicates that non-thermal factors' control on pCO_2 is greater than the

Formatted: Indent: Left: 0.2"

Formatted: English (United States)

Formatted: English (United States)

Commented [HX1]: What's this?

control from temperature. Tidal control on parameters was investigated using only the continuous monitoring data (Table 5). Hourly measurements of water level immediately offshore from the Aransas Ship Channel were obtained from NOAA's Tides and Currents Aransas Pass Station https://tidesandcurrents.noaa.gov/waterlevels.html?id=8775241&name=Aransas,%20Aransas%20Pass&state=TX. Tide data were merged with our sensor data by date and hour; given that there were gaps in available water level measurements (and no measurements prior to December 20, 2016), the usable dataset was reduced from 6088 observations to 5121 observations and fall was omitted from analyses. To examine differences between parameters during high tide and low tide, we defined high tide as tide level greater than the third quartile tide level value and low tide as a tide level less than the first quartile tide level value. The difference between high and low tide for each parameter was examined within each season (using t-tests) because of a significant interaction (based on $\alpha=0.05$) between the season and high/low tide factors in a two-way ANOVA.

Tidal control on parameters was investigated using our continuous monitoring data and tide level data obtained from NOAA's Aransas Pass Station (the Aransas Pass Station used for windspeed data, < 2 km offshore from monitoring location, Fig. 1) at https://tidesandcurrents.noaa.gov/waterlevels.html?id=8775241&name=Aransas,%20Aransas%20Pass&state=TX. Hourly measurements of water level were merged with our sensor data by date and hour. Given that there were gaps in available water level measurements (and no measurements prior to December 20, 2016), the usable dataset was reduced from 6088 observations to 5121 observations and fall was omitted from analyses. To examine differences between parameters during high tide and low tide, we defined high tide as tide level greater than the third quartile tide level value and low tide as a tide level less than the first quartile tide level value.

Other factors that may exert control on the carbonate system were investigated through parameter relationships. In addition to previously discussed tide and windspeed data, we obtained dissolved oxygen (DO), PAR, turbidity, and chlorophyll fluorescence data ~~were obtained~~ from MANERR-deployed environmental sensors that were co-located at our monitoring location (obtained from https://missionaransas.org/science/download-data). Given that MANERR data are all measured ~~at~~in the bottom water (>5 m) while our sensors were measuring surface waters, we excluded the observations with significant water column stratification (defined as a salinity difference > 3 between surface water ~~from our YSI~~ and bottom water ~~from the MANERR's YSI~~) from analyses. Omitting stratified water reduced our continuous dataset from 6088 to 5524 observations (removing 260 winter, 133 spring, 51 summer, and 120 fall observations), and omitting observations where there were no MANERR data to determine stratification further reduced the dataset to 4112 observations. Similarly, removing instances of stratification reduced discrete sample data from 104 to 89 surface water observations.

Formatted: Font: (Default) Times New Roman

Formatted: Kern at 12 pt

2.45 ~~Data Processing and~~ Statistical Analyses

Formatted: Font: 12 pt, Font color: Auto

Formatted: Heading 2, Indent: First line: 0"

Formatted: Font: Italic

All statistical analyses were performed in R, version 4.0.3 (R Core Team, 2020). To investigate differences between daytime and nighttime parameter values (temperature, salinity, pH, pCO_2, and CO_2 flux) using continuous monitoring data across the full sampling period and within each season, paired *t*-tests were used, pairing each respective day's daytime and nighttime values (Table S3). We also used loess models (locally weighted polynomial regression) to identify changes in diel patterns over the course of our monitoring period.

Two-way ANOVAs were used to examine differences in parameter means ~~(temperature, salinity, pH, pCO_2, and CO_2 flux)~~between seasons and between monitoring methods (Table S2). Since there were significant interactions (between season and sampling type factors) in the two-way ANOVAs for each individual parameter (Table S2), differences between seasons were investigated within each monitoring method (one-way ANOVAs) and the differences between monitoring methods were investigated within each season (one-way ANOVAs). For the comparison of monitoring methods, we included both the full discrete sampling data as well as a subset of the discrete sampling data to overlap with the continuous monitoring period (referred to throughout as reduced discrete data or D_C) along with the continuous data. To interpret differences between monitoring methods, a difference in means between the continuous monitoring and discrete monitoring datasets would only indicate that the 10-month period of continuous monitoring was not representative of the 5+ year period that discrete samples have been collected, but a difference in means between the continuous data and discrete sample data collected during the continuous monitoring period represents discrepancies between types of monitoring. Post-hoc multiple comparisons (between seasons within sampling types and between sampling types within seasons) were conducted using the Westfall adjustment (Westfall, 1997).

Differences in parameters between high tide and low tide conditions were investigated using a two-way ANOVA to model parameters based on tide level and

Formatted: Subscript

season. In models for each parameter, there was a significant interaction between tide level and season factors (based on α=0.05, results not shown), thus t-tests were used (within each season) to examine differences in parameters between high and low tide conditions. Note that f~~F~~all was omitted from this analysis because tide data were only available at the location beginning December 20, 2016. Sample sizes were the same for each parameter (High tide – winter: 354, spring: 569, summer: 350; Low tide – winter: 543, spring: 318, summer: 415).

Additionally, to gain insight to carbonate system controls through correlations, we conducted Pearson correlation analyses to examine individual correlations ~~between~~of pH and $p$$CO_2$ (both continuous and discrete) with other environmental parameters (Table S5).

To better understand overall system variability over different time scales, we used a linear discriminant ~~(LD)~~ analysis (LDA), a multivariate statistic that allows dimensional reduction, to determine the linear combination of environmental parameters (individual parameters reduced into linear discriminants, LDs) that allow the best differentiation between day and night as well as between seasons. We included $p$$CO_2$, pH, temperature, salinity, tide level, wind speed, total PAR, DO, turbidity, and fluorescent chlorophyll in this analysis. ~~This used the same suite of environmental data and data sources as Sect. 4.1.2.~~

All variables were centered and scaled to allow direct comparison of their contribution to the system variability. The magnitude (absolute value) of coefficients of the LDs (Table ~~7~~1) represents the relative importance of each individual environmental parameter in the best discrimination between day and night and between seasons, i.e., the

Formatted: Indent: First line: 0.5"

Formatted: Font: Italic

Formatted: Subscript

greater the absolute value of the coefficient, the more information the associated parameter can provide about whether the sample came from day or night (or winter, spring, or summer). Only one LD could be created for the diel variability (since there are only two classes to discriminate between – day and night). Two LDs could be created for the seasonal variability (since there were three classes to discriminate between – fall was omitted because of the lack of tidal data), but we chose to only report the coefficients for LD1 are reported (Table 7) given that LD1 captured 95.64% of the seasonal variability.

Tidal control on parameters was investigated using only the continuous monitoring data (Table 5). Hourly measurements of water level immediately offshore from the Aransas Ship Channel were obtained from NOAA's Tides and Currents Aransas Pass Station https://tidesandcurrents.noaa.gov/waterlevels.html?id=8775241&name=Aransas,%20Aransas%20Pass&state=TX. Tide data were merged with our sensor data by date and hour; given that there were gaps in available water level measurements (and no measurements prior to December 20, 2016), the usable dataset was reduced from 6088 observations to 5121 observations and fall was omitted from analyses. To examine differences between parameters during high tide and low tide, we defined high tide as tide level greater than the third quartile tide level value and low tide as a tide level less than the first quartile tide level value. The difference between high and low tide for each parameter was examined within each season (using t-tests) because of a significant interaction (based on α=0.05) between the season and high/low tide factors in a two-way ANOVA.

Other physical factors that may exert control on the carbonate system (including windspeed, salinity, tide level, and turbidity) can also be investigated through parameter relationships. We further investigated controls on the carbonate system using tide and

Formatted: Indent: First line: 0"

Formatted: Font: (Default) Times New Roman windspeed data (obtained from NOAA's Aransas Pass station at https://tidesandcurrents.noaa.gov/) and dissolved oxygen, PAR, turbidity, and chlorophyll fluorescence data (obtained from the MANERR at https://missionaransas.org/science/download-data) along with our continuous and discrete data. All investigations of relationships between environmental parameters discussed below included only the observations with no significant water column stratification (defined as a salinity difference of less than 3 between surface water from our YSI and bottom water (>5 m) from the MANERR's YSI). This omission of stratified water was intended to omit instances of substantial differences in chemical parameters between the surface and bottom water since all MANERR environmental data used in our analysis were measured at depth while our sensors measured surface water. Omitting stratified water reduced our continuous dataset from 6088 to 5524 observations (removing 260 winter, 133 spring, 51 summer, and 120 fall observations), and omitting observations where there were no MANERR data to determine stratification further reduced the dataset to 4112 observations. Similarly, removing instances of stratification reduced discrete sample data from 104 to 89 surface water observations.

Linear regression analysis within each season reveals that winter, spring, and fall all experience increases in pCO_2 with increasing wind, while there is not a significant relationship in summer.

To help examine controls on the carbonate system on a diel time scale, we used loess models (locally weighted polynomial regression) to identify changes in diel patterns over the course of our monitoring period (Fig. 8)

3. Results

3.1 ~~Continuous monitoring results~~Seasonal variability

Both the continuous and discrete data showed substantial seasonal variability for all parameters (Fig. 2, ~~(Fig. 2,~~ Tables S1 and S2). All discrete sample results reported here are for the entire 5+ years of monitoring; the subset of discrete sample data that overlaps with the continuous monitoring period will be addressed only in the discussion for method comparisons (Section 4.1.1). Both continuous and discrete data demonstrate significant differences in temperature between each season, with the highest temperature in summer and the lowest in winter (~~Fig. 2,~~ Tables S1 and S2). ~~For both continuous and discrete data, the m~~Mean salinity during sampling periods was highest in the summer and lowest in the fall Table S1). Significant differences in seasonal salinity occurred between all seasons except spring and winter for continuous data, but only summer differed from other seasons based on discrete data (Tables S1 and S2).

Carbonate system parameters also varied seasonally (Fig. 2). For both continuous and discrete data, winter had ~~both~~ the highest seasonal pH (8.19 ± 0.08 and 8.162 ± 0.065, respectively) and lowest seasonal pCO_2 (365 ± 44 µatm and 331 ± 39 µatm, respectively), while summer had ~~both~~ the lowest seasonal pH (8.05 ± 0.06 and 7.975 ± 0.046, respectively) and highest seasonal pCO_2 (463 ± 48 µatm and 511 ± 108, respectively) (Fig. 2, Table S1). All seasonal differences in pH and pCO_2 were significant ~~for continuous data and discrete data~~, except for the ~~the non-significant difference with~~ discrete data ~~between~~ spring ~~and~~versus fall for both parameters (Table S2).

Formatted: Font: Italic

Formatted: Subscript

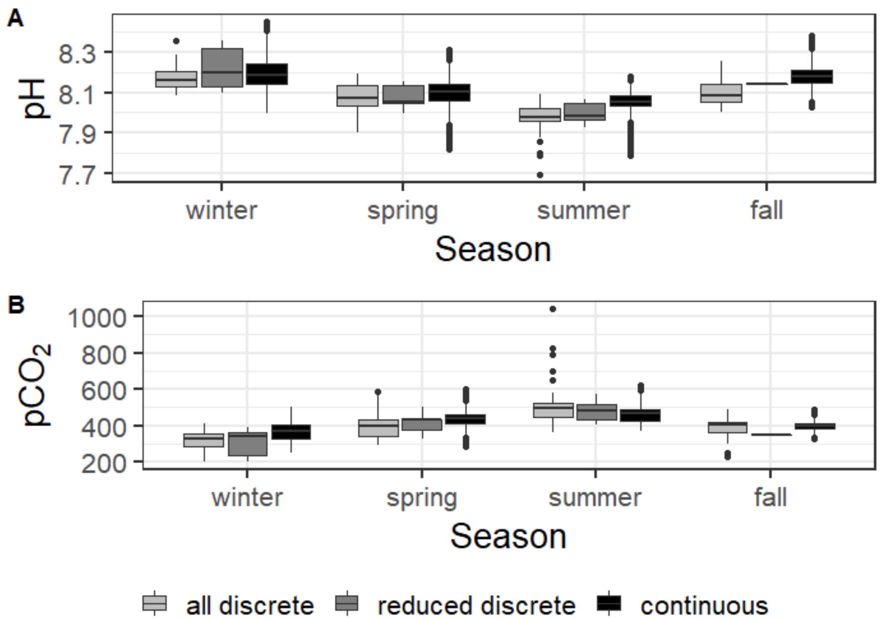

Figure 2. Boxplots of seasonal variability in pH and pCO_2 using all discrete data, reduced discrete data (to overlap with continuous monitoring, Nov. 8 2016 – Aug 23, 2017), and continuous sensor data.

~~The seasonally weighted mean CO_2 flux calculated from sensor data across the entire monitoring period was 0.2 ± 23.7 mmol m^{-2} d^{-1} (Table 1).~~ Mean CO_2 flux differed by season (Fig. 3, Tables S1 and S2~~-3)~~). Both continuous and discrete data records resulted in ~~Winter and fall both had~~ net negative CO_2 fluxes during fall and winter months, with winter being most negative. ~~(winter was most negative~~Both methods reported a net positive flux for summer, while spring fluxes were positive according to continuous data and negative according to the 5+ years of discrete data (Fig. 3, Table S1). ~~);~~ Annual net CO_2 fluxes were near zero (Table S1). ~~and summer and spring both had a net positive CO_2 flux (summer was most positive) (Table 1, Fig. 5). CO_2 flux also fluctuated on a daily scale, with the mean diel range (daily maximum – minimum) over~~

Formatted: Indent: First line: 0", Line spacing: single

Formatted: Subscript

the entire monitoring period being 34.1 ± 29.0 mmol m^{-2} d^{-1} (Table 2). However, there was not a significant difference in CO_2 flux calculated for daytime versus nighttime hours for the entire monitoring period or any individual season based on α=0.05 (paired t-test, Table 2).

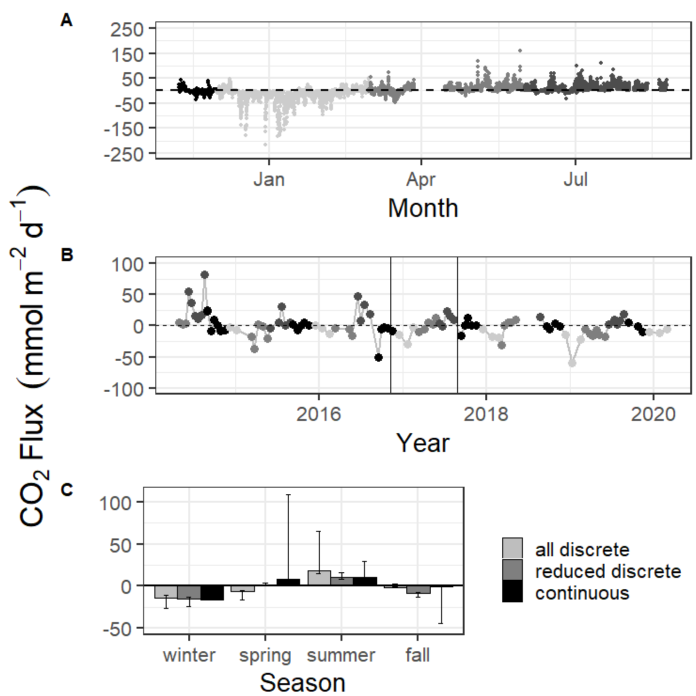

Figure 3. CO_2 flux calculated over the sampling periods from continuous (A) and discrete (B) data using the Jiang et al. (2008) wind speed parameterization. Gray scale in (A) and (B) denote different seasons. Vertical lines in (B) denote the time period of continuous monitoring. (C) shows the seasonal mean CO_2 flux. E calculated using the Jiang et al. (2008) gas transfer velocity parameterization and error bars representing mean CO_2 flux calculation using Ho (2006) and Raymond and Cole (2001) windspeed parameterizations.

Results of the LDA incorporated carbonate system parameters along with additional environmental parameters to get a full picture of system variability over seasonal timescales (Table 1). The most important parameter in system variability that allowed differentiation between seasons was temperature (Table 1, Seasonal LD1), as would be expected with the clear seasonal temperature fluctuations (Fig. S1-E). The second most important parameter for seasonal differentiation was chlorophyll, likely indicating clear seasonal phytoplankton blooms. The carbonate chemistry also played a critical role in seasonal differentiation, as pCO_2 was the third most important factor (Table 1).

Table 1. Coefficients of linear discriminants (LD) from LDA using continuous sensor data and other environmental parameters. Discriminants for both diel and seasonal variability shown.

	Seasonal	**Diel**
	LD1	**LD1**
Temperature (°C)	-3.53~~279~~	0.54~~06~~
Salinity	0.04~~32~~	0.15~~473~~
pCO_2 (μatm)	-0.29~~28~~	-0.16~~12~~
pH	0.10~~0991~~	0.06~~593~~
Tide Level (m)	-0.24~~389~~	0.10~~0968~~
Wind speed (ms^{-1})	0.05~~04~~	-0.00~~09~~
Total PAR	-0.07~~676~~	-2.29~~878~~
DO ($mg\ L^{-1}$)	0.09~~859~~	-0.08~~39~~
Turbidity	0.15~~455~~	-0.06~~561~~
Fluor. Chlorophyll	-0.40~~40~~	0.14~~397~~

3.2 Diel variability

The 10 months of in-situ continuous monitoring revealed that there was substantial diel variability in measured parameters (Fig. 4, Table S3). Temperature had a mean diel range of 1.3 ± 0.8°C (Table S3). Daytime and nighttime temperature differed significantly during the summer and fall months, with higher temperatures at night for both seasons (Table S3). ~~We note that significant differences in day and night temperature within seasons do not indicate that the diel difference were observed on all~~

Formatted: Font: Bold

Formatted: Font: (Default) Times New Roman

Formatted: Font: 10 pt

Formatted: Font: (Default) Times New Roman

Formatted: Font: Not Italic

Formatted: Normal, Line spacing: single days within the season, as large standard deviations in both daytime and nighttime values result in considerable overlap. The mean diel range of salinity was 3.4 ± 2.7 (Table S3). Daytime and nighttime salinity differed significantly during the winter and fall months, with higher salinities at night for both seasons. The mean diel range of pH was 0.09 ± 0.05 (Table S3). Daytime and nighttime pH differed significantly during the winter, summer, and fall, months; with nighttime pH was significantly higher than that of the daytime during the summer and winter months, and daytime pH was significantly higher during theand lower during fall (Fig. 4, Table S3). The mean diel range of pCO_2 was 58 ± 33 µatm (Fig. 4, Table S3). Daytime and nighttime pCO_2 differed significantly during the winter and summer months, with nighttime pCO_2 significantly higher during the summer and lower during the winter (Fig. 4, Table S3). N; nighttime pCO_2 was significantly higher than that of the daytime during the summer and daytime pCO_2 was significantly higher during the winter (Fig. 4, Table S3). Despite day-night differences in pCO_2, there was no significant difference in daytime and nighttime DO were observed during any season (Fig. 5F; paired t-tests, winter $p = 0.1573$, spring $p = 0.4877$, summer $p = 0.794$).

Loess models that investigated the evolution of day-night difference in parameters revealed that other environmental parameters, including salinity, temperature, and tide level, also had diel patterns thethat varied over the duration of our continuous monitoring (Fig. 5).

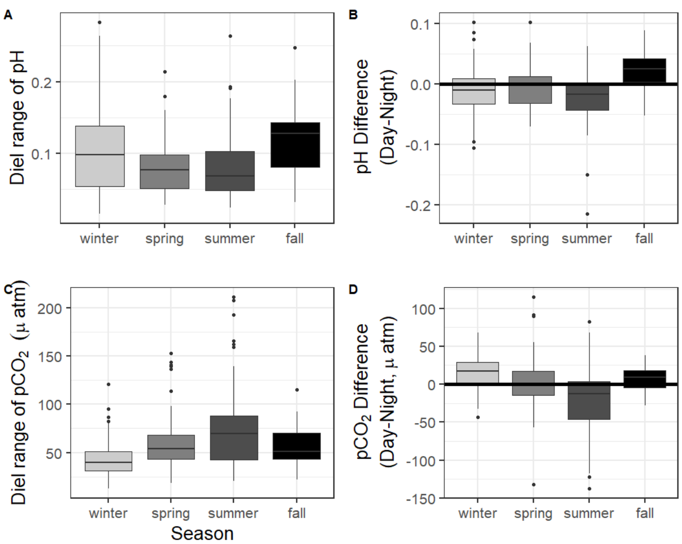

Figure 4. Boxplots of the diel range (maximum minus minimum) and difference in daily parameter mean daytime minus nighttime measurements for pH and pCO_2 from continuous sensor data.

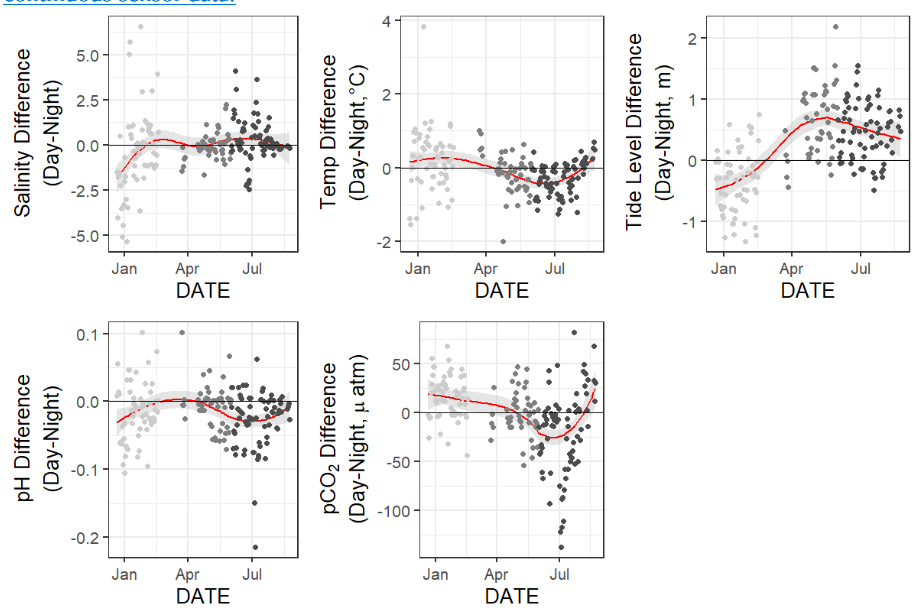

~~Figure 5. Loess models (red line) and their confidence intervals (gray bands) showing the difference in daily parameter mean daytime minus nighttime measurements.~~

~~The gray scale of the data points represents the four seasons over which data were collected~~

Formatted: Line spacing: single

CO_2 flux also fluctuated on a daily scale, with a mean diel range of 34.1 ± 29.0 mmol m^{-2} d^{-1} (Table S3). However, there was not a significant difference in CO_2 flux ~~calculated for d~~of daytime versus nighttime hours for the entire monitoring period or any individual season based on α=0.05 (paired t-test, Table S3).

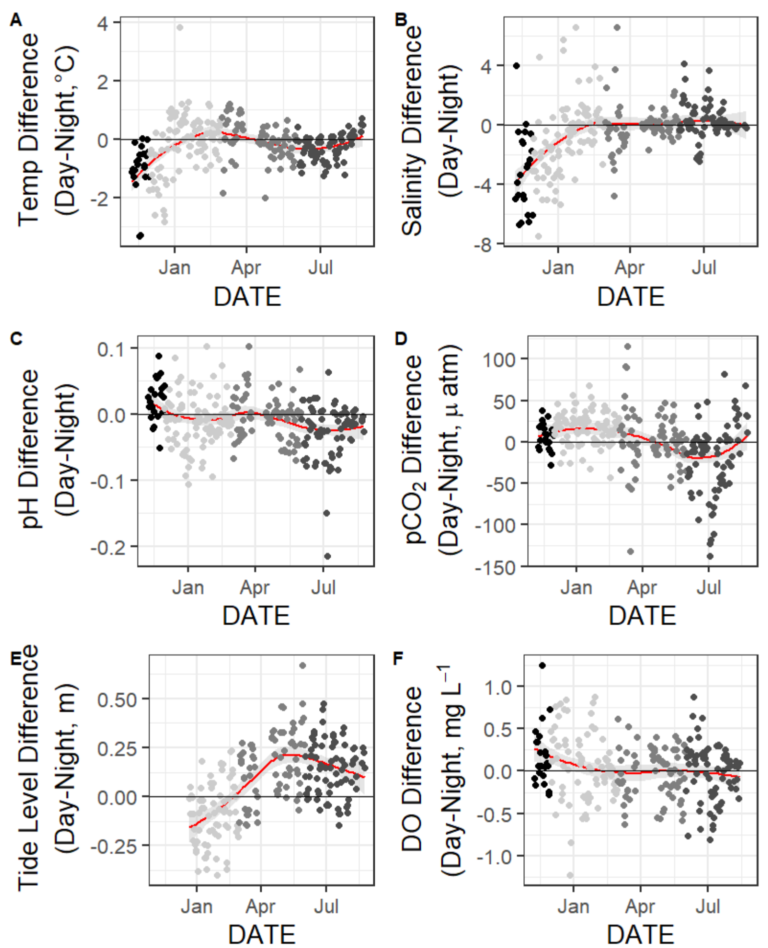

Figure 5. Loess models (red line) and their confidence intervals (gray bands) showing the difference in daily parameter mean daytime minus nighttime measurements. The gray scale of the data points represents the four seasons over which data were collected

Results of the LDA for differentiation between daytime and nighttime conditions revealed that the most important factor was PAR, as would be expected (Table 1, Diel LD1). Temperature was the second most important factor to differentiate between day and night. The carbonate chemistry also played a critical role in day/night differentiation, as pCO_2 was the third most important parameter, providing more evidence for differentiation between day and night than other parameters that would be expected to vary on a diel timescale (e.g., chlorophyll and DO) (Table 1).

3.3 Controlling factors and correlates

The relative influence of thermal and non-thermal factors (T/B) in controlling pCO_2 varied over different time scales (Fig. 6, Table S4~~Table 4~~2~~, Fig. 6~~). ~~T/B calculated from sensor data for the entire period was 0.98, indicating that the magnitude of control of non-thermal processes on pCO_2 was slightly greater than that of temperature~~Based on continuous data, non-thermal processes generally exerted more control tha~~t~~n thermal processes (T/B<1) over the entire 5+ years of discrete monitoring, within each season, and over most (167~~1~~/178) days (Fig. 6, Table S4~~Table 2~~). ~~Within seasons, T/B calculated from sensor data ranged from 0.51 in the winter to 0.69 in the spring, showing that non-thermal processes exert more control on pCO_2 within each individual season (Table 4). On a daily scale, only 11 of the 178 days with measurements for all 24 hours had temperature control of pCO_2 exceeding the non-thermal control (Table 4, Fig. 6).~~A~~For the entire 5+ years of discrete monitoring, non-thermal processes also exerted more~~

Formatted: Font: Not Italic

Formatted: Normal, Indent: First line: 0.5"

~~control than temperature on pCO_2. However, discrete data demonstrated that there was substantial interannual variability in T/B, with a~~nnual T/B from discrete data ranginged

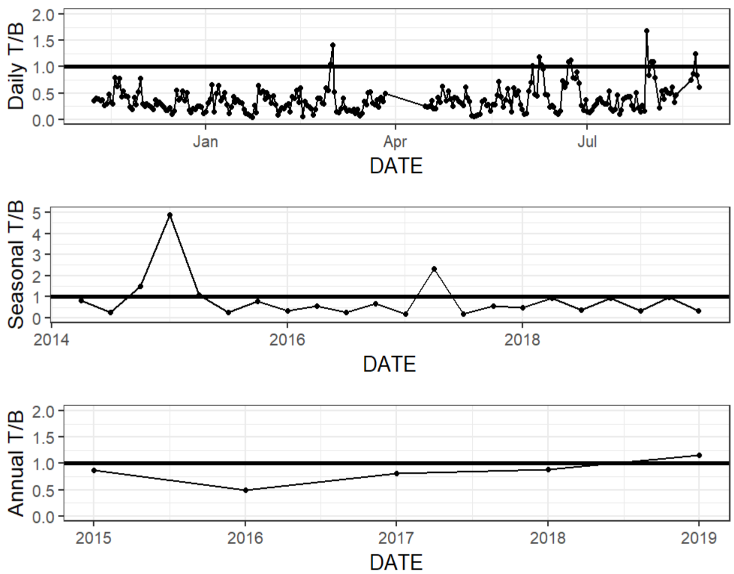

from 0.~~48~~50 to 1.16, with only one~~7 and two~~ of the five sampled years having T/B greater than one (i.e., more thermal influence; Table S4). While ~~the majority~~most ~~of~~ individual seasons that were sampled experienced stronger non-thermal control on pCO_2 (T/B <1), the only season that never experienced -stronger thermal control was summer, with summer T/B values ranging from 0.21 – 0.35 for the 6 sampled years (Table S4).

~~**Table 2.** Thermal versus non-thermal control on pCO_2 over different time scales using both continuous sensor data (C) and discrete sample data (D). If more than one segment of time is being considered (n>1), ΔpCO_2 values are the mean ± standard deviation of all segments, T/B range is the minimum and maximum T/B, and the number out of n with T/B>1 is recorded.~~

~~Time Period / Scale~~	~~Sampling type~~	~~n~~	~~$\Delta pCO_{2,thermal}$ (µatm)~~	~~$\Delta pCO_{2,nonthermal}$ (µatm)~~	~~T/B~~	~~Number out of n with T/B >1~~
~~Full Monitoring Period~~	~~D~~	~~1~~	~~301.9~~	~~537.8~~	~~0.56~~	

Formatted: Indent: First line: 0"

Formatted: Font: 12 pt

(May 2, 2014- Feb. 25, 2020)						
Annual	D	5	259.3 ± 16.0	319.1 ± 130.9	-0.48 – 1.17	2/5
Continuous Monitoring Period	C	1	355.0	360.7	0.98	
(Nov 2016 – August 2017)	D	1	236.3	229.9	1.03	
Winter	C	1	168.2	328.4	0.51	
	D	6	42.2 ± 23.4	101.7 ± 78.7	-0.20 – 4.90	1/6
Spring	C	1	171.4	246.9	0.69	
	D	6	142.3 ± 53.7	147.8 ± 67.3	-0.59 – 2.42	2/6
Summer	C	1	100.2	179.9	0.56	
	D	6	46.9 ± 26.6	176.9 ± 108.3	-0.21 – 0.35	0/6
Fall	C	1	105.9	181.6	0.58	
	D	6	179.8 ± 59.5	176.6 ± 78.1	-0.59 – 3.06	2/6
Daily	C	178	21.8 ± 11.8	63.8 ± 30.3	-0.05 – 1.68	11/178

Figure 6. Thermal versus non-thermal control on pCO_2 daily (top), seasonal (middle), and annual (bottom) time scales using both continuous sensor data (daily) and discrete sample data (seasonal and annual).

Tidal fluctuations seemed to have a significant effect on carbonate system parameters (Table 32). Both temperature and salinity were higher at low tide during the winter and summer months and higher at high tide during the spring. pCO_2 was higher during low tide during all seasons. pH was higher during high tide during the winter and summer, but this reversed during the spring, when pH was higher at low tide. CO_2 flux also varied with tidal fluctuations. CO_2 flux was higher (more positive or less negative) in the low tide condition for all seasons (though the difference was not significant in spring), i.e., the location was less of a CO_2 sink during low tide conditions in the winter and more of a CO_2 source during low tide conditions in the summer.

Table 3. Mean and standard deviation of temperature, salinity, pH, pCO_2, and calculated CO_2 flux (from continuous sensor measurements) during high and low tide conditions.

Parameter	**Season**	**High Tide Mean**	**Low Tide Mean**	**Difference between tide levels, t-test p-value**
Temperature (°C)	Winter	16.7 ± 1.7	17.6 ± 2.0	**<0.0001**

	Spring	24.4 ± 2.7	23.6 ± 2.7	**<0.0001**
	Summer	29.3 ± 0.5	30.1 ± 0.7	**<0.0001**
Salinity	Winter	30.2 ± 2.5	31.3 ± 2.9	**<0.0001**
	Spring	30.4 ± 1.9	30.0 ± 2.7	**0.0071**
	Summer	30.5 ± 2.4	34.5 ± 3.0	**<0.0001**
pH	Winter	8.20 ± 0.08	8.15 ± 0.06	**<0.0001**
	Spring	8.07 ± 0.09	8.10 ± 0.07	**<0.0001**
	Summer	8.08 ± 0.04	8.04 ± 0.06	**<0.0001**
***p*CO_2 (µatm)**	Winter	331 ± 40	378 ± 42	**<0.0001**
	Spring	435 ± 33	443 ± 50	**0.0154**
	Summer	419 ± 30	482 ± 48	**<0.0001**
CO_2 Flux (mmol m^{-2} d^{-1})	Winter	-33.0 ± 38.1	-11.7 ± 21.8	**<0.0001**
	Spring	7.4 ± 14.0	8.7 ± 14.8	**0.2248**
	Summer	1.8 ± 6.3	16.0 ± 14.5	**<0.0001**

Mean water level varied between all seasons; mean spring (highest) water levels were on average 0.08 m higher than winter (lowest) water levels (ANOVA p<0.0001, fall was not considered because of a lack of water level data). The mean daily tidal range during our continuous monitoring period was 0.39 m ± 0.13 m, which did not significantly differ between seasons (ANOVA p=0.739). However, the day-night difference in tide level exhibited a strong seasonality~~ pattern during the continuous monitoring period~~, with spring and summer having higher tide level during the daytime and winter having higher tide level during the nighttime (Fig. 5). ~~This same seasonal pattern in day-night difference in tide level is exhibited from Dec 20, 2016 (when the tide data is first available) through the rest of our discrete monitoring period (Feb 25, 2020), indicating that tidal control on diel variability of carbonate system parameters was likely consistent throughout this 3+ year period.~~

There were significant correlations between carbonate system parameters (pH and *p*CO_2) and many of the other environmental parameters, including windspeed, DO, turbidity, and fluorescent chlorophyll (~~Table S4~~Figure 7, Table S5). Both the continuous and discrete sampling types indicate that pH has a significant negative relationship with

Formatted: Indent: First line: 0"

Formatted: Font: Italic

Formatted: Subscript

both temperature and salinity and pCO_2 has a significant positive relationship with both temperature and salinity (Fig. 67). However, correlations with temperature were stronger for continuous data and correlations with salinity were stronger for discrete data (Table S45). The strongest correlations between continuous carbonate system data and all investigated environmental parameters were with DO (positive correlation with pH and negative correlation with pCO_2; Table S45). It is worth noting that there were no observations of hypoxia at our study site during our monitoring, with minimum DO levels of 3.9 mg L^{-1} and 4.0 mg L^{-1} for our continuous monitoring period and our discrete sampling period, respectively.

Formatted: Font: Italic

Formatted: Subscript

Formatted: Line spacing: single

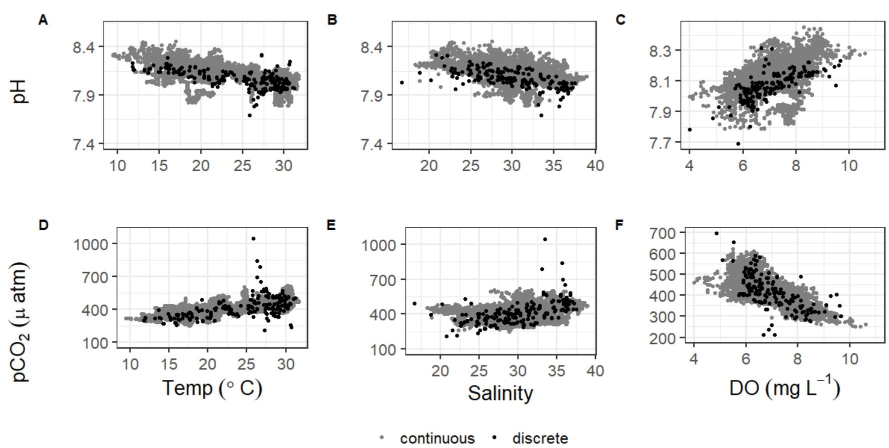

Figure 7. Correlations of pH and pCO_2 with temperature, salinity, and DO from continuous sensor data (gray) and all discrete data (black).

Over the 10-month continuous monitoring period, all sensor-measured parameters showed substantial temporal variability on seasonal and diel time scales (Fig. 2, Tables 1-

Formatted: Font: Not Italic

Formatted: Normal, Line spacing: single

3). Mean values of sensor-measured parameters over the entire monitoring period were: temperature – 23.1°C ± 5.3°C, ranging from 9.4°C to 31.7°C; salinity – 30.8 ± 3.7, ranging from 18.3 to 38.9; pH – 8.12 ± 0.10, ranging from 7.79 to 8.45; and pCO_2 – 416 ± 60 µatm, ranging from 251 µatm to 620 µatm (Table 1). Temperature was significantly different between each season (Table 3), with the highest being summer and the lowest being winter (Table 1). Salinity was highest in the summer and lowest in the fall, and salinity differed between all seasons except from spring and winter (Tables 1 and 3). pH and pCO_2 were both significantly different between all seasons (Table 3). Winter had both the highest seasonal pH (8.19 ± 0.08) and lowest seasonal pCO_2 (365 ± 44 µatm) and summer had both the lowest seasonal pH (8.05 ± 0.06) and highest seasonal pCO_2 (463 ± 48 µatm) (Table 1, Fig. 2–3).

Table 1. Mean and standard deviation of annual and seasonal temperature, salinity, pH, pCO_2, and CO_2 flux from continuous monitoring, discrete sampling over the continuous monitoring period, and discrete sampling over the entire sampled period. Reported annual means are seasonally weighted to account for disproportional sampling between seasons (however, reported annual standard deviation is associated with the un-weighted, arithmetic mean). CO_2 fluxes were calculated using the Jiang et al. (2008) wind speed parameterization for gas transfer velocity, and ranges of CO_2 flux that are given in brackets represent means calculated using parameterizations from Ho et al. (2006) and Raymond and Cole (2001), respectively.

Parameter		**Continuous Monitoring**	**Discrete Sampling**	
	Time Period	Nov. 8 2016 – Aug 23, 2017	Nov. 8 2016 – Aug 23, 2017	May 2, 2014–Feb. 25, 2020
Temperature (°C)	**Annual**	23.1 ± 5.3	23.5 ± 5.0	24.1 ± 5.3
	Winter	17.3 ± 2.1	17.3 ± 1.1	16.2 ± 2.0
	Spring	23.8 ± 2.8	23.4 ± 2.9	22.6 ± 3.7
	Summer	29.7 ± 0.8	29.6 ± 0.5	28.7 ± 1.4
	Fall	22.5 ± 2.1	23.6 ± 0.1	25.5 ± 4.5
Salinity	**Annual**	30.8 ± 3.7	30.4 ± 3.5	30.1 ± 4.4
	Winter	30.0 ± 3.7	29.3 ± 4.6	28.9 ± 2.9
	Spring	30.2 ± 2.6	30.0 ± 1.7	28.7 ± 3.4
	Summer	33.3 ± 3.2	33.6 ± 3.2	34.6 ± 2.8
	Fall	27.6 ± 3.7	28.8 ± 0.1	28.4 ± 4.5
pH	**Annual**	8.12 ± 0.10	8.092 ± 0.078	8.079 ± 0.092
	Winter	8.19 ± 0.08	8.157 ± 0.041	8.162 ± 0.065
	Spring	8.09 ± 0.09	8.078 ± 0.056	8.077 ± 0.066

Formatted: Font: (Default) Times New Roman

Formatted: Centered (×13)

	Summer	8.05 ± 0.06	7.999 ± 0.051	7.975 ± 0.046
	Fall	8.18 ± 0.05	8.136 ± 0.001	8.100 ± 0.071
pCO_2 (µatm)	**Annual**	416 ± 60	400 ± 71	406 ± 100
	Winter	365 ± 44	349 ± 31	331 ± 39
	Spring	436 ± 45	413 ± 54	396 ± 67
	Summer	463 ± 48	480 ± 59	511 ± 108
	Fall	400 ± 25	357 ± 2	386 ± 62
CO_2 Flux (mmol m^{-2} d^{-1})	**Annual**	**0.2 ± 23.7** [0.1 – (-87.6)]	**-1.5 ± 9.2** [(-2.6) – (-4.5)]	**(-0.8) ± 18.7** [(-0.7) – 5.3]
	Winter	**(-16.9) ± 29.2** [(-14.6) – (-444.0)]	**(-9.9) ± 5.2** [(-8.3) – (-16.2)]	**(-13.0) ± 13.5** [(-10.6) – (-25.6)]
	Spring	**7.6 ± 15.0** [6.5 – 109.0]	**1.0 ± 7.1** [1.0 – 3.3]	**(-6.5) ± 12.2** [(-5.5) – (-18.0)]
	Summer	**10.8 ± 13.3** [9.1 – 28.9]	**10.5 ± 7.8** [8.6 – 16.3]	**18.3 ± 19.6** [15.3 – 65.5]
	Fall	**(-0.9) ± 7.7** [(-0.7) – (-44.0)]	**(-7.5)** [(-6.2) – (-11.4)]	**(-2.3) ± 13.7** [(-1.9) – (-0.9)]

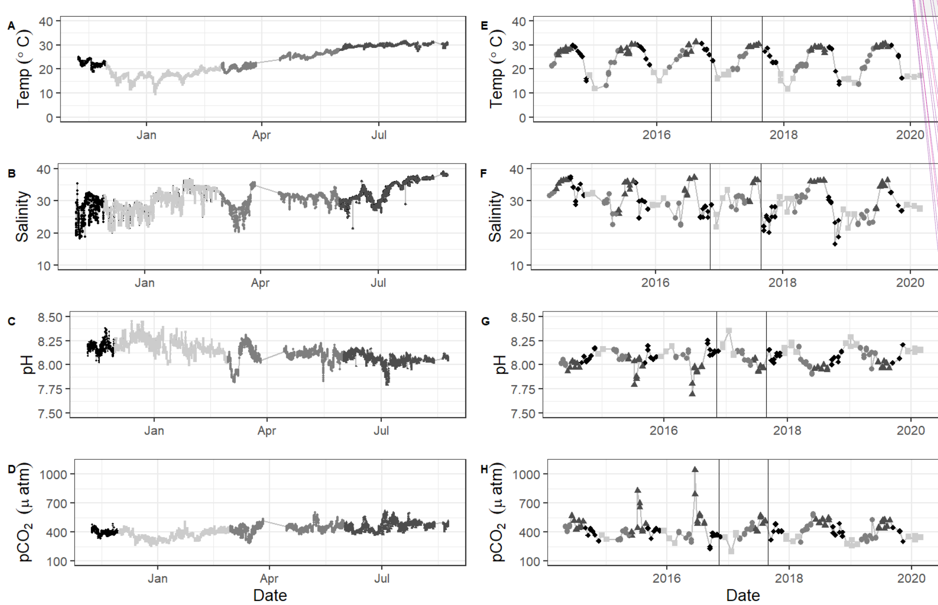

Fig 2. Time series data from continuous monitoring (A-D, Nov 8, 2016 to Aug 3, 2017) and discrete sample analysis (E-H, Nov 8, 2016 to Aug 3, 2017) at the Aransas Ship Channel. Gray scale (and shape) in the datapoints represents divisions between the four seasons. Vertical lines in (E-H) denote the time period of continuous monitoring.

Formatted: Centered
Formatted: Centered
Formatted: Centered
Formatted: Centered
Formatted: Centered
Formatted: Centered
Formatted: Centered
Formatted: Font: Bold
Formatted: Centered
Formatted: Font: Bold
Formatted: Font: Bold
Formatted: Font: Bold
Formatted: Centered
Formatted: Font: Bold
Formatted: Font: Bold
Formatted: Font: Bold
Formatted: Centered
Formatted: Font: Bold
Formatted: Font: Bold
Formatted: Font: Bold
Formatted: Centered
Formatted: Font: Bold
Formatted: Font: Bold
Formatted: Font: Bold
Formatted: Centered
Formatted: Font: Bold
Formatted: Font: Bold

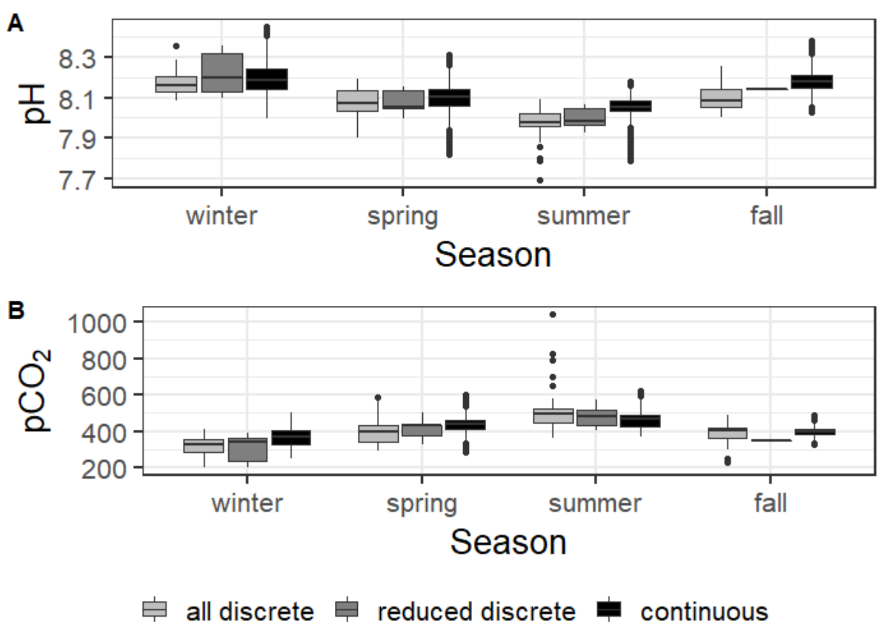

Figure 32. Boxplots of seasonal variability in pH and pCO_2 using all discrete data (May 2, 2014–Feb. 25, 2020), reduced discrete data (Nov. 8 2016 – Aug 23, 2017, to overlap with continuous monitoring, Nov. 8 2016 – Aug 23, 2017), and continuous sensor data. (Nov. 8 2016 – Aug 23, 2017)

Table 2. Diel variability in system parameters from continuous sensor data (Nov 8, 2016 – Aug 23, 2017). The p-values reported are from a paired *t* test comparing the means of each day (9am-3pm LST) with the mean of the same night (9pm – 3am LST); all significant results based on α=0.05 are bolded. Diel range calculations were done using only days with the full 24 hours of hourly measurements (176 out of 262 measured) to ensure that data gaps did not influence the calculations. Reported fluxes use the Jiang et al. (2008) gas transfer velocity parameterization. Note that the Fall season had much fewer observations than other seasons because of the timing of sensor deployment.

Parameter	**Time Period**	**Daytime Mean**	**Nighttime Mean**	**Day versus Night p-value**	**Mean Diel Range**	**Minimum Diel Range**	**Maximum Diel Range**
Temperature (°C)	**Full Sampling Period**	23.0 ± 5.3	23.2 ± 5.4	**<0.0001**	1.3 ± 0.8	0.30	3.93
	Winter	17.2 ± 2.1	17.4 ± 2.1	0.2055	1.5 ± 0.8	0.3	3.8
	Spring	23.7 ± 2.7	23.8 ± 2.9	0.5579	1.2 ± 0.6	0.3	3.0
	Summer	29.6 ± 0.7	29.9 ± 0.8	**<0.0001**	1.0 ± 0.6	0.3	3.8
	Fall	22.0 ± 1.19	23.0 ± 1.0	**<0.0001**	1.8 ± 0.9	0.8	3.9

Salinity	**Full Sampling Period**	30.5 ± 4.1	31.0 ± 3.3	**0.0004**	3.4 ± 2.7	0.250	15.870
	Winter	29.6 ± 4.2	30.4 ± 3.1	**0.0051**	3.8 ± 2.2	0.25	9.48
	Spring	30.1 ± 2.6	30.2 ± 2.6	0.5604	2.5 ± 2	0.4	8.17
	Summer	33.4 ± 3.2	33.1 ± 3.3	0.0550	2.0 ± 1.7	0.3	9.73
	Fall	25.9 ± 3.9	29.0 ± 3.2	**<0.0001**	7.7 ± 3.6	1.2	15.87
pH	**Full Sampling Period**	8.12 ± 0.10	8.13 ± 0.09	**<0.0001**	0.09 ± 0.05	0.02	0.28
	Winter	8.18 ± 0.08	8.20 ± 0.07	**0.0108**	0.10 ± 0.05	0.02	0.28
	Spring	8.09 ± 0.09	8.10 ± 0.08	0.3286	0.08 ± 0.03	0.03	0.18
	Summer	8.04 ± 0.06	8.07 ± 0.05	**<0.0001**	0.08 ± 0.04	0.03	0.19
	Fall	8.20 ± 0.05	8.17 ± 0.05	**0.0038**	0.12 ± 0.04	0.03	0.20
***p*CO_2 (µatm)**	**Full Sampling Period**	417 ± 54	416 ± 65	0.7065	58 ± 33	12.6	211.3
	Winter	374 ± 44	358 ± 43	**<0.0001**	43 ± 21	12.6	121.1
	Spring	438 ± 42	437 ± 48	0.7237	61 ± 31	20.5	152.8
	Summer	452 ± 44	471 ± 51	**0.0003**	74 ± 42	23.6	211.3
	Fall	406 ± 24	399 ± 27	0.0545	56 ± 18	22	92.2
CO_2 Flux (mmol m^{-2} d^{-1})	**Full Sampling Period**	0.0 ± 6.3	-1.3 ± 5.9	0.3028	34.1 ± 29.0	2.7	189.0
	Winter	-14.9 ± 8.4	-19.1 ± 7.7	0.0676	46.6 ± 38.9	2.7	189.0
	Spring	7.6 ± 5.2	7.0 ± 5.2	0.6680	27.5 ± 18.5	4.9	115.0
	Summer	9.4 ± 5.6	11.7 ± 5.2	0.1167	32.3 ± 22.9	4.5	111.0
	Fall	0.1 ± 3.8	-0.3 ± 3.5	0.7449	17.0 ± 10.2	3.9	40.1

Formatted: Indent: First line: 0"

Table 3. Tests examining differences in mean carbonate system parameters between seasons and between types of sampling (continuous monitoring with sensors Nov. 8 2016 – Aug 23, 2017, discrete sample collection and laboratory measurement during only the continuous monitoring period Nov. 8 2016 – Aug 23, 2017, and discrete sample collection and laboratory measurement during the entire sampling period May 2, 2014-Feb. 25, 2020). For both the two-way ANOVA and associated one-way ANOVAs, p-values are listed. All significant results based on α=0.05 are bolded, and the F statistic is in parentheses. Since all two-way ANOVAs had a significant interaction between factors, individual one-way ANOVAs were conducted for each level of the other factor. Following significant one-way ANOVAs, multiple comparisons using the Westfall adjustment (Westfall, 1997) were conducted; individual comparisons with significantly different means (based on α=0.05) are listed as unequal beneath the one-way ANOVA results (All ≠ indicates that every individual comparison between levels had significantly different means. W = winter, Sp = spring, Su = summer, F = fall; C = continuous sensor data, D = discrete sample data over the entire discrete monitoring period, D_C = Discrete sample data during only the period of continuous monitoring).

Parameter	**Two-way ANOVA**			**One-way ANOVA and post-hoc multiple comparison results for differences between types of sampling**				**One-way ANOVA and post-hoc multiple comparison results for difference between seasons**		
	Interaction	Season	Sampling type	winter	spring	summer	fall	Continuous	Discrete	Discrete

									(Continuous Period)	(Entire Period)
Temp (°C)	**<0.0001** (15.8)	**<0.0001** (12369.7)	0.7346 (0.3)	0.0710 (2.6)	0.1052 (2.3)	**<0.0001** (19.6) D≠C	**<0.0001** (61.4) D≠C	**<0.0001** (12559) All≠	**<0.0001** (22.8) W≠Su; W≠Sp; W≠F; Su≠Sp; Su≠F	**<0.0001** (58.2) All≠
Salinity	**0.0141** (2.7)	**<0.0001** (598.7)	0.6509 (0.4)	0.1716 (1.8)	**0.0013** (6.7) D≠C	0.1921 (1.7)	0.7007 (0.4)	**<0.0001** (580.0) W≠Su; W≠F; Su≠Sp; Su≠F; Sp≠F	0.2516 (1.6)	**<0.0001** (17.5) W≠Su; Su≠Sp; Su≠F
pH	**0.0013** (3.7)	**<0.0001** (1412.3)	**<0.0001** (24.0)	0.4026 (0.9)	0.9238 (0.1)	**<0.0001** (24.1 D≠C **C≠Dc**	**<0.0001** (33.2) D≠C	**<0.0001** (1381.2) All≠	**0.0152** (5.7) W≠Su	**<0.0001** (35.3) W≠Su; W≠Sp; W≠F; Su≠Sp; Su≠F
***p*CO_2 (μatm)**	**<0.0001** (10.4)	**<0.0001** (1747.3)	**0.0147** (4.2)	**0.0018** (6.4) D≠C	**<0.0001** (17.4) D≠C	**0.0002** (8.4) D≠C	0.0398 (3.2) **All=**	**<0.0001** (1737.6) All≠	**0.0407** (4.0) W≠Su	**<0.0001** (8.4) W≠Su; W≠Sp; W≠F; Su≠Sp; Su≠F
CO_2 Flux (mmol m^{-2} d^{-1})	**0.0144** (2.6)	**<0.0001** (738.1)	0.6739 (0.4)	0.9140 (0.1)	**<0.0001** (11.8) D≠C	**0.0214** (3.9) D≠C	0.5849 (0.5)	**<0.0001** (725.9) All≠	**0.0299** (4.5) W≠Su	**<0.0001** (19.2) W≠Su; W≠F; Su≠Sp; Su≠F

There was substantial diel variability in parameters (Table 2, Fig. 4). Over the 10-month in-situ monitoring period, temperature had a mean diel range (daily maximum minus daily minimum) of 1.3 ± 0.8°C (Table 2). Daytime and nighttime temperature differed significantly during the summer and fall months, with higher temperatures at night for both seasons (Table 2). The mean diel range of salinity was 3.4 ± 2.7 (Table 2). Daytime and nighttime salinity differed significantly during the winter and fall months, with higher salinities at night for both seasons. The mean diel range of pH was 0.09 ± 0.05 (Table 2). Daytime and nighttime pH differed significantly during the winter, summer, and fall months; nighttime pH was significantly higher than that of the daytime during the summer and winter months, and daytime pH was significantly higher during the fall (Table 2, Fig. 4). The mean diel range of *p*CO_2 was 58 ± 33 µatm (Table 2, Fig. 4). Daytime and nighttime *p*CO_2 differed significantly during the winter and summer months; nighttime *p*CO_2 was significantly higher than that of the daytime during the summer and daytime *p*CO_2 was significantly higher during the winter (Table 2, Fig. 4).

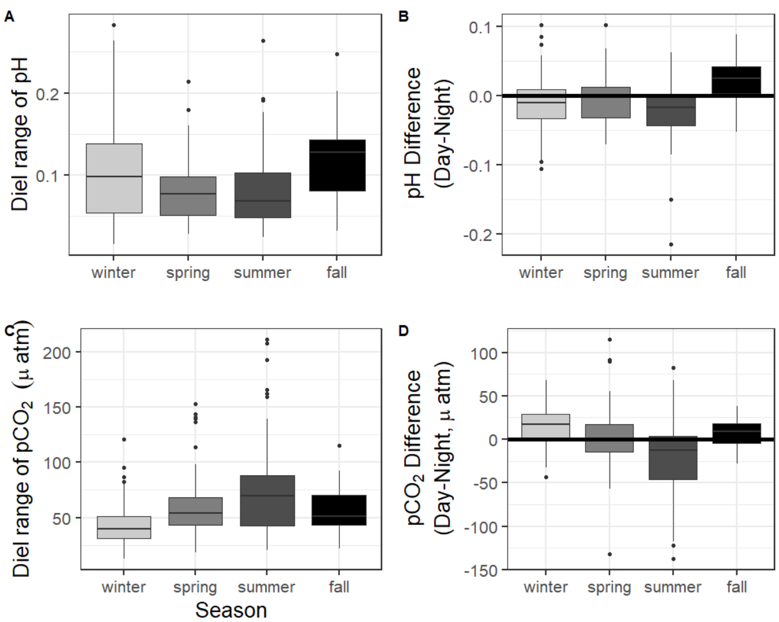

Figure 4 3. Boxplots showing of the diel range (maximum minus minimum) and difference in daily parameter mean daytime minus nighttime measurements for pH and *p*CO_2 from continuous sensor data.

The seasonally weighted mean CO_2 flux calculated from sensor data across the entire monitoring period was 0.2 ± 23.7 mmol m^{-2} d^{-1} (Table 1). Mean CO_2 flux differed by season (Table 3). Winter and fall both had net negative CO_2 flux (winter was most negative), and summer and spring both had a net positive CO_2 flux (summer was most positive) (Table 1, Fig. 5). CO_2 flux also fluctuated on a daily scale, with the mean diel range (daily maximum – minimum) over the entire monitoring period being 34.1 ± 29.0 mmol m^{-2} d^{-1} (Table 2). However, there was not a significant difference in CO_2 flux calculated for daytime versus nighttime hours for the entire monitoring period or any individual season based on α=0.05 (paired t-test, Table 2).

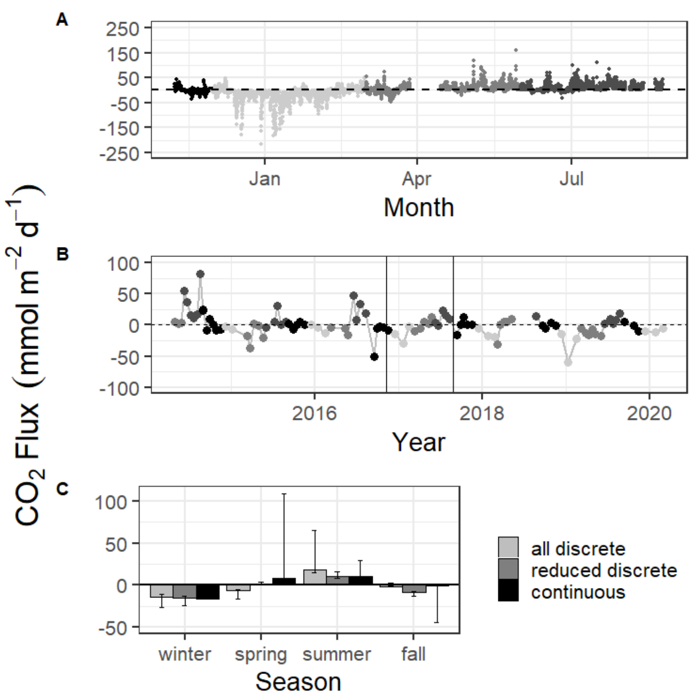

Figure 45. CO_2 flux calculated over the sampling periods from continuous (A) and discrete (B) data using the Jiang et al. (2008) wind speed parameterization. Gray scale in (A) and (B) denote different seasons. Vertical lines in (B) denote the time period of continuous monitoring. (C) shows the seasonal mean CO_2 flux calculated using the Jiang et al. (2008) gas transfer velocity parameterization and error bars representing mean CO_2 flux calculation using Ho (2006) and Raymond and Cole (2001) windspeed parameterizations. The different color bars within each season represent all discrete data (May 2, 2014- Feb. 25, 2020), reduced discrete data (Nov. 8 2016 – Aug 23, 2017, to

overlap with continuous monitoring), and continuous sensor data (Nov. 8 2016 – Aug 23, 2017).

The relative influence of thermal and nonthermal factors (T/B) in controlling pCO_2 varied over different time scales (Table 4, Fig. 6). T/B calculated from sensor data for the entire period was 0.98, indicating that the magnitude of control of non-thermal processes on pCO_2 was slightly greater than that of temperature. Within seasons, T/B calculated from sensor data ranged from 0.51 in the winter to 0.69 in the spring, showing that non-thermal processes exert more control on pCO_2 within each individual season (Table 4). On a daily scale, only 11 of the 178 days with measurements for all 24 hours had temperature control of pCO_2 exceeding the non-thermal control (Table 4, Fig. 6).

Table 4. Thermal versus non-thermal control on pCO_2 (Takahashi et al. 2002) over different time scales using both continuous sensor data (C) and discrete sample data (D) (indicated as Sampling Type C and D, respectively). If more than one segment of time is being considered (n>1), ΔpCO_2 values are the mean ± standard deviation of all segments, the T/B values arerange is the minimum and maximum T/B, and the number out of n with T/B>1 (indicating greater control of pCO_2 by temperature than other processes) is recorded. The summary of annual T/B values from discrete data includes only 2015-2019 (n=5 years; 2014 and 2020 were omitted since monitoring did not occur throughout the entire year). Daily values from continuous data were only reported for those days with all 24 measurements.

Time Period / Scale	Sampling type	n	$\Delta pCO_{2,\,thermal}$ (µatm)	$\Delta pCO_{2,\,nonthermal}$ (µatm)	T/B	Number out of n with T/B >1
Full Monitoring Period (May 2, 2014–Feb. 25, 2020)	D	1	301.9	537.8	0.56	
Annual	D	5	259.3 ± 16.0	319.1 ± 130.9	0.48 – 1.17	2/5
Continuous Monitoring Period (Nov 2016 – August 2017)	C	1	355.0	360.7	0.98	
	D	1	236.3	229.9	1.03	
Winter	C	1	168.2	328.4	0.51	
	D	6	42.2 ± 23.4	101.7 ± 78.7	0.20 – 4.90	1/6
Spring	C	1	171.4	246.9	0.69	
	D	6	142.3 ± 53.7	147.8 ± 67.3	0.59 – 2.42	2/6
Summer	C	1	100.2	179.9	0.56	
	D	6	46.9 ± 26.6	176.9 ± 108.3	0.21 – 0.35	0/6
Fall	C	1	105.9	181.6	0.58	
	D	6	179.8 ± 59.5	176.6 ± 78.1	0.59 – 3.06	2/6
Daily	C	178	21.8 ± 11.8	63.8 ± 30.3	0.05 – 1.68	11/178

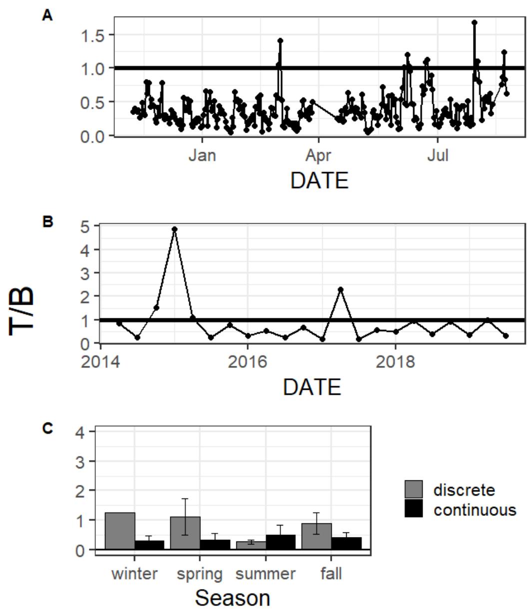

Figure 6. T/B (thermal *p*CO_2/ non-thermal *p*CO_2) calculated for each day from continuous (A) and each season from discrete (B) data. Bar graphs showing the seasonal mean and standard deviation of T/B from both discrete and continuous data (C).

Mean water level varied between all seasons; mean spring (highest) water levels were on average 0.08 m higher than winter (lowest) water levels (ANOVA $p<0.0001$, fall was not considered because of a lack of water level data). Tidal influence on pH was less clear. Data from continuous monitoring did not show a significant correlation between pH and tide level across the entire monitoring period (Table 6). Significant differences in mean pH between tide levels were recorded during each season; pH was higher at high tide (corresponding with the lower *p*CO_2) during the winter and summer, but pH was lower at high tide (conflicting with the lower *p*CO_2) in the spring (Table 5). Tidal fluctuations had a significant effect on carbonate system parameters (Table 5). Both temperature and salinity were higher at low tide during the winter and summer months and higher at high tide during the spring. pH was higher at high tide during the winter and summer and higher at low tide during the spring, and *p*CO_2 was higher during low tide during winter, spring, and summer (Table 5). CO_2 flux also varied with tidal fluctuations. CO_2 flux was higher in the low tide condition for all season with tide data; the location was less of a CO_2 sink during low tide conditions in the winter and more of a CO_2 source during low tide conditions in the spring and summer. The mean daily tidal fluctuation during our continuous monitoring period was 0.39 m ± 0.13 m, which did not significantly differ between seasons (ANOVA p=0.739). However, diel patterns in tidal fluctuations exhibited a strong seasonal pattern during the continuous monitoring period, with spring and summer having higher tide level during the daytime and winter having higher tide level during the nighttime (Fig. 8). This same seasonal pattern in diel tidal fluctuations is exhibited from Dec 20, 2016 (when the tide data is first available) through the rest of our discrete monitoring period (Feb 25, 2020), indicating that tidal control on diel variability of carbonate system parameters was likely consistent throughout this time period.There were no observations of hypoxia at our study site during our monitoring, with minimum DO levels of 3.9 mg L^{-1} and 4.0 mg L^{-1} for our continuous monitoring period and our discrete sampling period, respectively.

Table 5. Differences in temperature, salinity and mean carbonate system parameters from continuous sensor data between high tide and low tide. High tide was defined as a tide level greater than Q3 and low tide was defined as a tide level less than Q1. Seasons were examined separately with t-tests because of a significant interaction (based on α=0.05) between the season and high/low tide factors in a two-way ANOVA. Fall was omitted from the analysis because tide data was only available at the location beginning December 20, 2016.

Parameter	Season	High Tide Mean	Low Tide Mean	Difference between tide levels,

Formatted Table

				t-test p-value
Temperature (°C)	Winter	16.7 ± 1.7	17.6 ± 2.0	**<0.0001**
	Spring	24.4 ± 2.7	23.6 ± 2.7	**<0.0001**
	Summer	29.3 ± 0.5	30.1 ± 0.7	**<0.0001**
Salinity	Winter	30.2 ± 2.5	31.3 ± 2.9	**<0.0001**
	Spring	30.4 ± 1.9	30.0 ± 2.7	**0.0071**
	Summer	30.5 ± 2.4	34.5 ± 3.0	**<0.0001**
pH	Winter	8.20 ± 0.08	8.15 ± 0.06	**<0.0001**
	Spring	8.07 ± 0.09	8.10 ± 0.07	**<0.0001**
	Summer	8.08 ± 0.04	8.04 ± 0.06	**<0.0001**
***p*CO_2 (µatm)**	Winter	331 ± 40	378 ± 42	**<0.0001**
	Spring	435 ± 33	443 ± 50	**0.0154**
	Summer	419 ± 30	482 ± 48	**<0.0001**
CO_2 Flux (mmol m^{-2} d^{-1})	Winter	-33.0 ± 38.1	-11.7 ± 21.8	**<0.0001**
	Spring	7.4 ± 14.0	8.7 ± 14.8	**0.2248**
	Summer	1.8 ± 6.3	16.0 ± 14.5	**<0.0001**

3.2 Discrete sampling results

All results reported here are for the entire 5+ years of monitoring; the subset of discrete sample data that overlaps with the continuous monitoring period will be addressed only in the discussion for method comparisons. All reported discrete sampling parameters showed substantial temporal variability over the 5+ years of monitoring (Fig. 2E-H). The mean temperature was 24.1 ± 5.3°C, ranging from 11.8 – 31.2°C; the mean salinity was 30.1 ± 4.4, ranging from 16.7 – 37.5; the mean pH was 8.079 ± 0.092, ranging from 7.693 to 8.354; and the mean *p*CO_2 was 406 ± 100 µatm, ranging from 199 to 1043 (Table 1). These parameters all experienced significant seasonal variability (Tables 1 and 3). Temperature was significantly different between each season, highest in summer and lowest in winter (Tables 1 and 3). Salinity was highest during the summer months and was not significantly different between other seasons (Tables 1 and 3). pH and *p*CO_2 were both significantly different between all seasons with the exception of spring and fall (Table 3). Winter had both the highest seasonal pH (8.162 ± 0.065) and lowest seasonal

Formatted: Indent: First line: 0"

pCO_2 (331 ± 39 µatm), and summer had both the lowest seasonal pH (7.975 ± 0.046) and highest seasonal *p*CO_2 (511 ± 108) (Tables 1 and 3, Fig. 3).

Average annual CO_2 flux calculated with discrete sample data was slightly negative (-0.9± 18.7 mmol m^{-2} d^{-1}, Table 1). CO_2 flux varied greatly by season. Summer, the only season with a net positive CO_2 flux over the 5+ year period, had significantly higher flux than all other seasons; winter had the lowest calculated flux, but it was not significantly different from spring (Tables 1 and 3).

As with the continuous data, T/B calculated from the discrete data varied over different time scales (Table 4, Fig. 6). For the entire period, T/B was 0.56, indicating that non-thermal processes exerted more control than temperature on *p*CO_2. The annual T/B varied from 0.48 to 1.17, with two of the five sampled years having T/B greater than one (i.e. more thermal influence). While the majority of individual seasons that were sampled experienced stronger non-thermal control on *p*CO_2 (T/B <1), the only season that never experienced stronger thermal control was summer, with summer T/B values ranging from 0.21 – 0.35 for the 6 sampled years (Table 4).

As would be expected, we found that PAR provided the most differentiation between daytime and nighttime conditions (based on the largest coefficient associated with Diel LD1, Table 7). Temperature was the second most important factor in differentiating between day and night; this corresponds to the diel variability that we detected where both summer and fall had clear separation of mean temperature between day and night, with nighttime temperatures being 0.3 and 1.0 higher, respectively (Table 3). The next most important parameter in differentiating between day and night in this system was *p*CO_2, providing more evidence for differentiation between day and night than other parameters that would be expected to vary on a diel timescale (e.g. chlorophyll and DO). As for system variability that allowed differentiation between the four seasons, the most important parameter in system variability was temperature (Table 7, Seasonal LD1), as would be expected with the clear seasonal temperature fluctuations (Fig. 2E). The second most important parameter in contributing to seasonal variability was chlorophyll, likely indicating clear seasonal blooms. The third most important parameter for seasonal differentiation was pCO_2; therefore pCO_2 variability seems to be more closely tied to seasons than variability in tide level, DO, or the array of other parameters (Table 7). The contribution of pH to discriminating along diel or seasonal scales was less than pCO_2 despite the same seasonal differences that were identified by ANOVA (Table 3) and more seasons with significant diel differences (Table 2). However, pH still seemed to be relatively important on seasonal scales, having clearer contribution to seasonal system variability than several other parameters including DO and salinity.

Formatted: Indent: First line: 0"

Table 3. Coefficients of linear discriminants (LD) from LDA using continuous sensor data and other environmental parameters. Discriminants for both diel and seasonal variability shown.

	Diel LD1	**Seasonal LD1**
Temperature (°C)	0.5406	-3.5279
Salinity	0.1473	0.0432
pCO_2 (µatm)	-0.1612	-0.2928
pH	0.0593	0.0991
Tide Level (m)	0.0968	-0.2389
Wind speed (ms^{-1})	-0.0009	0.0504
Total PAR	-2.2878	-0.0676
DO ($mg\ L^{-1}$)	-0.0839	0.0859
Turbidity	-0.0561	0.1455

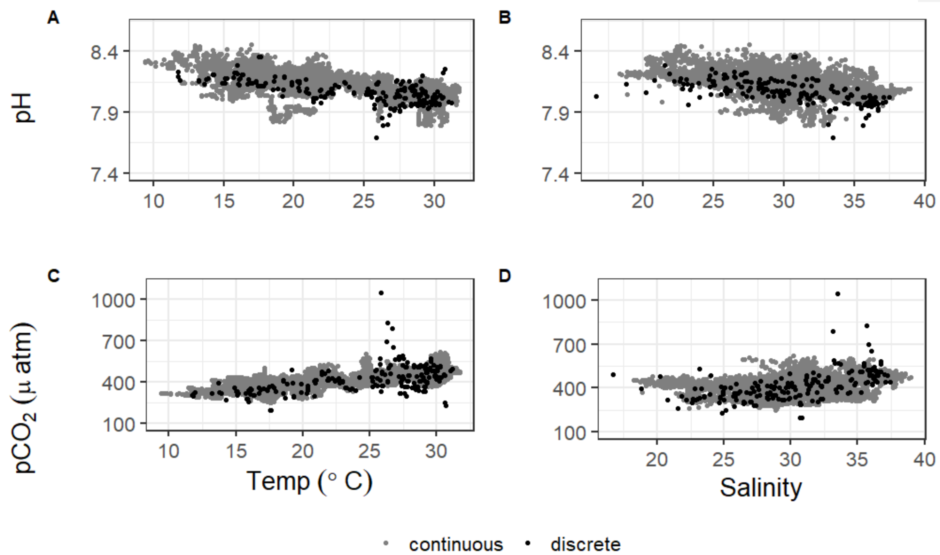

~~**Figure 6.** Correlations of pH and pCO_2 with temperature and salinity from continuous sensor data (gray) and all discrete data (black).~~

Formatted: Font: Bold

Formatted: Indent: First line: 0"

4. Discussion

4.1 Comparing continuous monitoring and discrete sampling: Representative sampling in a temporally variable environment

~~*4.1.1 Representative sampling in a temporally variable environment*~~

Discrete water sample collection and analysis is the most common method that has been employed to attempt to understand the carbonate system of estuaries. However, it is difficult to know if these samples are representative of the spatial and temporal variability in carbonate system parameters. While this time-series study cannot conclude whether our broader sampling efforts in the MAE are representative of the spatial variability in the estuary, it can investigate how representative our bimonthly to monthly sampling is of the more high-frequency temporal variability that the Aransas Ship ChannelASC experiences.

There were several instances where seasonal parameter means significantly differed between the 10-month continuous monitoring period and the 5+ year discrete sampling period (Table S2, C $\neq$ D or $D_c \neq$ D) including temperature in the summer and fall, salinity in the spring, pH in the summer and fall, and pCO_2 in winter, spring, and summer. While clear seasonal variability was demonstrated for most parameters (using both continuous and discrete data for the entire period), these differences between the 10-month continuous monitoring period and our 5+ year monitoring period illustrate that there is also interannual variability in the system. Therefore, short periods of monitoring are unable to fully capture current baseline conditions.

During the continuous monitoring period (2016-2017), we found no significant difference between sampling methods in the seasonal mean temperature, salinity, or pCO_2. The two sampling methods also resulted in the same mean pH for all seasons except for summer, when the sensor data recorded a higher mean pH than discrete samples (Tables S1 and S2). During this case, we can conclude that discrete monitoring did not accurately represent the system variability that was able to be captured by the sensor monitoring. However, given that most seasons did not show differences in pH or pCO_2 between sampling methods, the descriptive statistics associated with the discrete monitoring did a fair job of representing system means. This is evidence that long-term discrete monitoring efforts, which are much more widespread in estuarine systems than sensor deployments, can be generally representative of the system despite known temporal variability on shorter time scales. However, further study would be needed to determine if this applies throughout the system, as the upper estuary generally experiences greater variability.

Understanding the relationships of pH and pCO_2 with temperature and salinity is important in a system (Fig. 76). Both the continuous and discrete sampling types indicate that pH has a significant negative relationship with both temperature and salinity and pCO_2 has a s significant positive relationship with both temperature and salinity (Fig. 7). Based on the results of an Analysis of Covariance (ANCOVA), the relationship (slope) of pH with both temperature and salinity and of pCO_2 with salinity were not significantly different between types of monitoring (considering the sensor deployment period only), supporting the effectiveness of long-term discrete monitoring programs when sensors are unable to be deployed. However, ANCOVA did reveal the relationship of pCO_2 with temperature is significantly different (method:temp $p=0.0062$) between monitoring methods.

While continuous monitoring data from sensors is usually lacking substantial spatial coverage, it is effective in capturingThe high temporal resolution of sensor data is and presumably better for estimating providing better estimates of average CO_2 flux at a given location versusthan periodicdiscrete sampling. Previous studies have pointed out that discrete sampling methods, which generally involve only daytime sampling, do not adequately capture the diel variability in the carbonate system and may therefore lead to underestimation of CO_2 fluxes. However, we found no significant difference (within any season) between CO_2 flux values calculated with sensor data versus discrete samples (Table S32, Fig. 3). Calculated CO_2 fluxes also did not significantly differ between day and night during any season, despite some differences in pCO_2 (Table 2S3), likely due to the large error associated with the calculation of CO_2 flux (Table S1, Fig. 3) which will be further discussed below. Therefore, the expected underestimation of CO_2 flux based on diel variability of pCO_2 was not encountered at our study site, validating the use of discrete samples for quantification of CO_2 fluxes (until methods with less associated error are available). Even given less error in calculated flux, estimated fluxes would likely not differ between methods on an annual scale (as pCO_2 did not), but CO_2 fluxes may differ on a seasonal scale since the differences between daytime and nighttime pCO_2 were not consistent across seasons (Table ~~2~~S3, Fig. 4).

There are many factors contributing to error associated with CO_2 flux. There is still large error associated with estimates of estuarine CO_2 flux because turbulent mixing is difficult to model and turbulence is the main control on CO_2 gas transfer velocity, *k*, in shallow water environments. Thus, our wind speed parameterization of *k* is imperfect and likely the greatest source of error. Other notable sources of error include the data treatment. For example, we chose to seasonally weight the individual calculated flux values in the calculation of annual flux to account for differences in sampling frequency between seasons. From continuous data, the weighted average flux was 0.2 mmol m^{-2} d^{-1}, although choosing not to seasonally weight and simply look at the arithmetic mean of fluxes calculated directly from sampling dates would have resulted in an annual CO_2 flux of -0.7 mmol m^{-2} d^{-1} for the same period. Similarly, the weighted average flux from all 5+ years of discrete data was -0.9 mmol m^{-2} d^{-1}, but the arithmetic mean of fluxes would have resulted in an annual CO_2 flux of 0.2 mmol m^{-2} d^{-1} for the same period. Another source of error that could be associated with the calculation of flux from the discrete data is the way in which wind speed data are aggregated to be used in the windspeed parameterization. We decided to use daily averages of the windspeed for calculations. Using the windspeed measured for the closest time to our sampling time or the monthly averaged wind speed may have resulted in very different flux values.

4.1.2 Direct agreement of measurement methods and quantified uncertainties associated with parameters

Direct comparisons were made between measurements from sensors and laboratory-analyzed bottle samples – including both quality control (QC) samples taken from the cooler that housed the sensors at the time when these sensors took recorded readings and long-term monitoring samples taken from the ship channel near the sensors (within 100 m) that occurred at various times and were compared to sensor measurements of the closest full hour (Table 8). The mean difference between the SeaFET pH measurements and the QC samples (continuous – discrete) prior to sensor data correction was 0.05 ± 0.08 (Table 8, which would reduce to 0.00 ± 0.08 following the correction). The mean difference between the SAMICO2 pCO_2 measurements and the QC samples (continuous – discrete) was -18 ± 44 (Table 8) when discrete sample pCO_2 was calculated using Millero (2010) constants. We used several different constants to calculate pCO_2 to check this offset; all were similar in mean and standard deviation, but the offset could be slightly reduced using Millero (2002) constants.

Table 4. Comparison of discrete and continuous monitoring. The difference between sampling methods is reported in two different ways: the difference between sensor measurements and laboratory measurement of quality control (QC) bottle samples taken directly from the cooler (here the pH difference is prior to the sensor pH correction of +0.05), and the difference between sensor measurements and laboratory measurement of discrete samples taken from a nearby station for our 5+ year monitoring (here the pH difference is after the sensor pH correction of +0.05, see methods for details). For all calculated parameters, dissociation constants from Millero 2010 were used. Error – analytical error for directly measured parameters and propagated error for calculated parameters (mean ± standard deviation) – is also reported.

Commented [m2]: Xinping – I was considering moving this whole section to the supplemental materials to cut down on the total length. What do you think?

	Difference between sampling methods (mean difference ± standard deviation of the difference)		Error (Analytical or Propagated)	
	Sensor – QC cooler samples (prior to sensor pH correction, n=12)	Sensor – discrete samples (after pH sensor correction, n=13)	**Discrete Sampling (n = 104)**	**Continuous Monitoring (n = 6088)**
Temperature (°C)			0.1	0.1
Salinity	-0.16 ± 1.44	0.50 ± 1.69	0.01	0.1
pH	-0.05 ± 0.08	0.01 ± 0.12	0.0004	0.05
***p*CO_2 (µatm)**	-18 ± 44	25 ± 63	7 ± 2	1.0
DIC (µmol kg^{-1})			2.5	327.4 ± 63.2
TA (µmol kg^{-1})			7.4 ± 0.9	400.7 ± 81.0
Ω_{Ar}			0.19 ± 0.03	1.08 ± 0.31

Given that the analytical accuracy of the SeaFET instrument is 0.05 pH units, the average offset between sensor and laboratory values of quality control samples demonstrates fair agreement (Table 8). Given that calculated uncertainty associated with calculated discrete *p*CO_2 was 7 ± 2, we did not see great agreement between SAMICO2 *p*CO_2 and laboratory-calculated *p*CO_2 for quality control samples (mean difference of -18 ± 44, Table 8). Mean offsets and their associated standard deviations were larger when comparing sensor data to samples taken during our long-term discrete monitoring effort. This is not surprising given that the discrete sample collection did not occur at the exact time of the sensor measurement or the exact location of the cooler pump inlet. Greater sensor-laboratory agreement has been achieved for open ocean settings, but this larger standard deviation is likely a result of the temporal variability in the more complex estuarine environment where these instruments have been much less widely deployed to date.

Propagated error associated with calculated carbonate system parameters was calculated using the *seacarb* package in R (Gattuso et al., 2018) using analytical errors associated with the measurements of the input pair, *in situ* temperature and salinity, total boron, and the key dissociation constants (Table 8). Error associated with calculated parameters from discrete bottle samples was relatively small and likely a result of uncertainties in constants (Orr et al., 2018), but error associated with parameters calculated from sensor data was relatively large (Table 8). This large error is likely a result of both the relatively low analytical precision associated with the pH sensor and the poor mathematical combination of variables for speciation calculations. The high error suggests that it will be important that autonomous sensors that can measure alternative parameters and allow for lower propagated error are developed and broadly used to gain a full understanding of carbonate chemistry on high-frequency timescales.

4.21 Factors controlling temporal variability in carbonate system parameters

Our study site had a relatively small range of pH and pCO_2 on both diel and seasonal scales compared to other coastal regions (Challener et al., 2016; Yates et al., 2007). This small variability is likely tied to a combination of the subtropical setting (small temperature variability), the lower estuary position of our monitoring (further removed from the already small freshwater influence), little ocean upwelling influence, and the system's relatively high buffer capacity that results from the high alkalinity of the freshwater endmembers (Yao et al., 2020). Just as the extent of hypoxia-induced acidification was relatively low in Corpus Christi Bay because of the bay's high buffer capacity (McCutcheon et al., 2019), the extent of pH fluctuation resulting from all controlling factors at ASC would also be modulated by the region's high intrinsic buffer capacity.*4.21.1 Thermal versus non-thermal control of pCO_2*

Formatted: Font: Not Bold

Formatted: Normal, Line spacing: single

Formatted: Not Highlight

Formatted: Not Highlight

~~Substantial variability in the carbonate system was observed at the study site over multiple time scales including diel, seasonal, and interannual. Many physical and biological factors (e.g., temperature, currents, tides, wind speed, net ecosystem metabolism, etc.) can exert control on pCO_2 and subsequently exert control on other carbonate system parameterscarbonate chemistry. Using the thermal versus non-thermal analysis of control on *p*CO_2 from Takahashi et al. (2002), w~~We ~~were able to determine~~demonstrated that both temperature and non-thermal processes exert control on *p*CO_2, but non-thermal control generally surpasses thermal control ~~exert more control on the *p*CO_2~~ in ~~the Aransas Ship Channel~~ASC ~~relative to temperature~~ over multiple time scales (Fig. 6, Table S4~~Table 4~~2, T/B<1). The magnitude of *p*CO_2 variation attributed to non-thermal processes varied greatly (i.e., $\Delta pCO_{2,nt}$ had large standard deviations, Table ~~2~~S4). For example, during the year of strongest non-thermal control (2016), $\Delta pCO_{2,nt}$ was 53~~8~~4 µatm versus $\Delta pCO_{2,nt}$ of 20~~8~~9 µatm in the year of weakest thermal control (2019). Conversely, the magnitude of *p*CO_2 variation attributed to temperature was consistent across time scales. For example, during the year of strongest thermal control (2015), $\Delta pCO_{2,t}$ was 276 µatm versus $\Delta pCO_{2,t}$ of 24~~3~~2 µatm in the year of weakest thermal control (201~~9~~7). Spring and fall seasons, which experienced the greatest temperature swings (Table S1), had greater relative temperature control exerted on *p*CO_2 out of all seasons (Fig. 6, Table S4~~Table 2~~). The difference in T/B between sampling methods is relatively small over the 10-month sensor deployment period, but it is worth noting that T/B did not align over shorter seasonal time scales sampling methods (Fig. 6, Table ~~2~~S4). Continuous monitoring demonstrated a greater magnitude of fluctuation resulting from both temperature and non-thermal processes (i.e., greater– $\Delta pCO_{2,t}$ and $\Delta pCO_{2,nt}$),

Formatted: Not Highlight
Formatted: Not Highlight
Formatted: Not Highlight
Formatted: Not Highlight
Formatted: Font: Italic, Not Highlight
Formatted: Not Highlight
Formatted: Subscript, Not Highlight
Formatted: Not Highlight
Formatted: Not Highlight
Formatted: Not Highlight
Formatted: Not Highlight
Formatted: Not Highlight
Formatted: Not Highlight
Formatted: Not Highlight
Formatted: Not Highlight
Formatted: Not Highlight
Formatted: Not Highlight
Formatted: Not Highlight
Formatted: Not Highlight
Formatted: Not Highlight
Formatted: Not Highlight
Formatted: Not Highlight
Formatted: Not Highlight
Formatted: Not Highlight
Formatted: Not Highlight
Formatted: Not Highlight

indicating that the extremes are generally not captured by the discrete, daytime sampling, and sensor data would provide a better understanding of system controls.

~~Though annual average pCO_2 and CO_2 flux are higher in the upper estuary and lower offshore than at our study site, the same seasonal pattern of elevated pCO_2 and positive CO_2 flux in the summer and depressed pCO_2 and negative CO_2 flux during the winter observed at our site has also been observed throughout the entire MAE and in the open Gulf of Mexico (Hu et al., 2018; Yao and Hu, 2017).~~

The greater influence of non-thermal controls that we report conflicts with Yao and Hu (2017), who found that ASC was primarily thermally controlled (T/B 1.53 – 1.79) from May 2014 to April 2015. Yao and Hu (2017) also found that locations in the upper estuary experienced lower T/B during flooding conditions than drought conditions. Although the opposite was found at ASC, it is likely that the high T/B calculated at ASC by Yao and Hu (2017) was still a result of the drought condition due to the long residence time of the estuary. Since 2015, there has not been another significant drought in the system, so it seems that non-thermal controls on pCO_2 are more important at this location under normal freshwater inflow conditions.

Formatted: Not Highlight

Formatted: Not Highlight

Significantly warmer water temperatures were observed during the nighttime in both summer and fall (Fig. 5), indicating that temperature could exert a slight control on the carbonate system over a diel time scale. We note that significant differences in day and night temperature within seasons do not indicate that diel differences were observed on all days within the season, as large standard deviations in both daytime and nighttime values result in considerable overlap. More substantial temperature swings between seasons would result in more temperature control over a seasonal timescale. ASC seems to have less thermal control of the carbonate system than offshore GOM waters, as temperature had substantially higher explanatory value for pH and pCO_2 based on simple linear regressions in offshore GOM waters (R^2 = 0.81 and 0.78, respectively (Hu et al., 2018)) than at ASC (R^2 = 0.30 and 0.52, respectively, for sensor data and R^2 = 0.38 and 0.25, respectively, for discrete data).

Though annual average pCO_2 (and CO_2 flux) are higher in the upper MAE and lower offshore than at our study site, the same seasonal patterns that we observed (i.e., elevated pCO_2 and positive CO_2 flux in the summer and depressed pCO_2 and negative CO_2 flux during the winter, Table S1, Fig. S1) has also been observed throughout the entire MAE and the open Gulf of Mexico (Hu et al., 2018; Yao and Hu, 2017). These seasonal patterns correspond with both the directional response of the system to temperature and net community metabolism response to changing temperature, i.e., elevated respiration in summer months (Caffrey, 2004). Despite that there were no observations of hypoxia, there was a strong relationship between the carbonate system parameters and DO (Fig. 7, Table S45), suggesting that net ecosystem metabolism may exert an important control on the carbonate system on certain time scales. The lack of day-night difference in DO (Fig. 5F) despite the significant day-night difference in both pH and pCO_2 suggests that net community metabolism is likely not a strong controlling factor on diel time scales. Biological control likely becomes more important over seasonal timescales.

Formatted: Not Highlight

Formatted: Not Highlight

Formatted: Not Highlight

Formatted: Not Highlight

While the tidal range in the northwestern GOM is relatively small (1.30 m over our 10-month continuous monitoring period), the tidal inlet location of our study site results in proportionally more “coastal water” during high tide and proportionally more "estuarine water" during low tide. The carbonate chemistry signal of these different water masses was seen in the differences between high tide and low tide conditions at ASC (i.e., high tide having lower pCO_2 because coastal waters are less heterotrophic than estuarine waters, Table 32). Consequently, the relative importance of thermal versus non-thermal controls may be modulated by tide level. We calculated the thermal and non-thermal pCO_2 terms separately during high tide and low tide periods and found that non-thermal control is more important during low tide conditions (within each season T/B is 0.10 ± 0.07 lower during the low tide than high tide). This is likely because low tide has proportionally more "estuarine water" at the location and because there is less volume of water for the end products of biological processes to accumulate. The difference in T/B between high tide and low tide conditions was greatest in the spring, likely due to a combination of elevated spring-time productivity and larger tidal ranges in the spring.

Only five of 24 seasons (one winter, two spring, and two fall) throughout the years of discrete sampling had greater variability in pCO_2 attributed to temperature ($\Delta pCO_{2,\ thermal}$) than other processes ($\Delta pCO_{2,\ nonthermal}$) (Table 4). The magnitude of pCO_2 variation attributed to non-thermal processes varied greatly over multiple time scales (i.e. $\Delta pCO_{2,\ nonthermal}$ had large standard deviations, Table 42). For example, during the year of strongest non-thermal control (2016), $\Delta pCO_{2,\ nonthermal}$ was 538 µatm versus $\Delta pCO_{2,\ nonthermal}$ of 208 µatm in the year of weakest thermal control (2019). For example, in 2016 pCO_2 had the strongest non-thermal control of any year, with a $\Delta pCO_{2,\ nonthermal}$ of 538 µatm, while 2019 had the weakest control from non-thermal processes of any year, with a $\Delta pCO_{2,\ nonthermal}$ of 208. Conversely, the magnitude of pCO_2 variation attributed to temperature was consistent across time scales. For example, during the year of strongest

Formatted: Font: Italic, Not Highlight

Formatted: Not Highlight

Formatted: Subscript, Not Highlight

Formatted: Not Highlight

Formatted: Not Highlight

Formatted: Not Highlight

Formatted: Pattern: Clear

Formatted: Pattern: Clear (Background 1)

~~thermal control (2015), $\Delta p CO_{2,\ thermal}$ was , in 2015 pCO_2 had the strongest thermal control of any year, with a $\Delta pCO_{2,\ thermal}$ of 276 µatm, versus $\Delta pCO_{2,\ thermal}$ of 243 µatm in the year of weakest thermal control (2019). Spring and fall seasons, which experienced the greatest temperature swings (Table S1), had greater relative temperature control exerted on pCO_2 out of all seasons (Table 4). while 2019 had the weakest thermal control of any year, with a $\Delta pCO_{2,\ thermal}$ of 243 µatm.~~ The GOM is one of the few places in the world that experiences diurnal tides (Seim et al., 1987; Thurman, 1994), so theoretically, the fluctuations in pCO_2 associated with tides may align to either amplify or reduce/reverse the fluctuations that would result from diel variability in net community metabolism. Based on diel tidal fluctuations at this site (i.e., higher tides during the day in the spring and summer and higher tides at night during the winter, Fig. 5E)~~,~~ and the higher pCO_2 associated with low tide (Table 2), tidal control should amplify the biological signal (nighttime $pCO_2 >$ daytime pCO_2) during spring and summer and reduce or reverse the biological signal during the winter. This tidal control can explain the diel variability present in our pCO_2 data, which showed the full reversal of the expected biological signal in the winter (Fig. 5C, Table S3, nighttime $pCO_2 <$ daytime pCO_2), i.e., the higher nighttime tides in winter brought in enough low CO_2 water from offshore to fully offset any nighttime buildup of CO_2 from the lack of photosynthesis. However, we note that the expected diel, biological control was likely minimal since daytime DO was not consistently higher than nighttime DO (Fig. 5F). The same seasonal pattern diel tide fluctuations were exhibited from Dec 20, 2016 (when the tide data is first available) through the rest of our discrete monitoring period (Feb 25, 2020), indicating that tidal control on diel variability of carbonate system parameters was likely consistent

Formatted: Pattern: Clear (Background 1), Not Highlight

Formatted: Pattern: Clear (Background 1), Not Highlight

Formatted: Pattern: Clear (Background 1), Not Highlight

Formatted: Not Highlight

Formatted: Not Highlight

Formatted: Not Highlight

throughout this 3+ year period. The diel variability in pH did not mirror pCO_2 as would be expected (Fig. 5). The relationship between pH and tide level more closely mirrored the relationships of salinity and temperature with tide level (versus pCO_2 relationship with tide level; Table 2), indicating that controlling factors of the carbonate system may not be exerted equally on both pH and pCO_2 over different time scales.

tidal control should amplify the biological control signal (nighttime pCO_2 > daytime pCO_2) during spring and summer and reduce or reverse the biological control signal during the winter. This was supported by our pCO_2 data, which showed nighttime pCO_2 significantly greater than daytime pCO_2 in the summer, as expected from the biological signal (Table S3, Fig. 5). The full reversal of the biological signal in the winter (Table S3, nighttime pCO_2 < daytime pCO_2) indicated that tidal control exceeded biological control (i.e., the higher tides at nighttime in winter brought in enough low CO_2 water from offshore to fully offset the nighttime buildup of CO_2 from lack of photosynthesis during nighttime hours). The diel variability in pH did not mirror pCO_2 as would be expected. The loess models show that pCO_2 closely follows the directional response to both tide level and temperature, while pH does not (Fig. 5), indicating that controlling factors of the carbonate system may not be exerted equally on both pH and pCO_2 over different time scales.

Formatted: Not Highlight

The difference in T/B between sampling methods is relatively small over the 10-month sensor deployment period, but sampling methods did not align over shorter seasonal time scales (Table 42). Each method suggested temperature and nonthermal processes exert a relatively similar control on pCO_2, but cContinuous monitoring demonstrated a greater magnitude of fluctuation resulting from both temperature and non-thermal processes (i.e. greater $\Delta pCO_{2, thermal}$ and $\Delta pCO_{2, nonthermal}$),. Over shorter time scales, like individual seasons, the calculated T/B did not align well between sampling methods. The T/B (calculated using only data from Nov 2016 – August 2017) for discrete versus continuous sampling was respectively 0.17 versus 0.51 for winter, 2.37 versus 0.69 for spring, and 0.20 versus 0.56 for summer (Table 4, Fall was omitted since there was only one discrete sampling event during the fall of the continuous monitoring period). Sampling bias due to the small number of within-season sampling events for the discrete monitoring likely resulted in this difference. From both continuous and discrete data, summers always had stronger control exerted on pCO_2 from nonthermal processes than temperature. While temperatures were high during the summer months, the within-season variability in temperature was the lowest (Table 1); less of a temperature swing resulted in less thermal control on the system. Conversely, spring and fall seasons, which experienced the greatest temperature swings (Table 1), had greater relative temperature control exerted on pCO_2 (Table 4). The differences in $\Delta pCO_{2, thermal}$ and $\Delta pCO_{2, nonthermal}$ between monitoring methods illustrate that there is information that is missed when only sampling bimonthly/monthly and during the daytime. Generally, both $\Delta pCO_{2, thermal}$ and $\Delta pCO_{2, nonthermal}$ are higher when calculated from sensors than discrete sampling, indicating that the extremes are generally not captured by the discrete, daytime sampling, and sensor data would provide a better understanding of system controls.

The relative importance of thermal versus non-thermal controls may be modulated by tide level. ; we calculated the thermal and non-thermal pCO_2 terms separately during high tide and low tide periods to better investigate control via other physical and biological processes. The influence of tides can be removed from the calculated non-thermal pCO_2 term, leaving only biological processes and other physical controls in the non-thermal term, by examining periods of high tide and low tide separately. Using our sensor data and the same water level data used for the tide analysis, wWe found that T/B is higher (by 0.10 ± 0.07) during the high tide condition within each season. T/B for high tide and low tide, respectively, was 0.60 and 0.52 for winter, 0.84 and 0.66 for spring, and 0.62 and 0.58 for summer. The higher control exerted by nonthermal processes during low tide seems intuitive given that there is less volume of water for the end products of biological processes to build up in. The difference in T/B between high tide and low tide conditions was greatest in the spring, likely due to a combination of elevated spring-time productivity and larger tidal ranges in the spring.

Using data from the first year of our discrete sampling (May 2014 – April 2015), Yao and Hu (2017) reported that the Aransas Ship Channel T/B was 1.53 during drought and 1.79 during a period of flooding, both of which are significantly higher than what we found over most timescales (the exception being certain individual seasons, mostly during that first year of sampling, Table 42, Fig. 6B). Yao and Hu (2017) also found that locations in the upper estuary experienced lower T/B during flooding conditions than drought conditions, but the opposite was found for the Aransas Ship Channel location, where the flooding conditions had higher T/B. It is likely that the high T/B calculated by Yao and Hu (2017) was a result of the drought condition at the beginning of their sampling; given the long residence time of MAE, the Aransas Ship Channel may not have experienced the influence of the freshwater inflow by the end of the Yao and Hu

(2017) study. Once the freshwater reached the Aransas Ship Channel location, it would likely experience a reduced T/B as did the upper parts of the system. Since then, there has not been another significant drought in the system, so it seems as though the non-thermal controls on *p*CO_2 are more important at this location under normal freshwater inflow conditions.

4.21.2 Investigating controls on the carbonate system using relationships between carbonate system parameters and other environmental parameters

We further investigated controls on the carbonate system using tide and windspeed data (obtained from NOAA's Aransas Pass station at https://tidesandcurrents.noaa.gov/) and dissolved oxygen, PAR, turbidity, and chlorophyll fluorescence data (obtained from the MANERR at https://missionaransas.org/science/download-data) along with our continuous and discrete data. All investigations of relationships between environmental parameters discussed below included only the observations with no significant water column stratification (defined as a salinity difference of less than 3 between surface water from our YSI and bottom water (>5 m) from the MANERR's YSI). This omission of stratified water was intended to omit instances of substantial differences in chemical parameters between the surface and bottom water since all MANERR environmental data used in our analysis were measured at depth while our sensors measured surface water. Omitting stratified water reduced our continuous dataset from 6088 to 5524 observations, and omitting observations where there were no MANERR data to determine stratification further reduced the dataset to 4112 observations. Similarly, removing instances of stratification reduced discrete sample data from 104 to 89 surface water observations.

To extend upon the above discussion of thermal versus non-thermal controls on pCO_2, the extent of thermal control on both pH and pCO_2 can be investigated based on relationships between parameters. There is a strong negative correlation between pH and temperature and a strong positive correlation between pCO_2 and temperature (Table 6, Fig. 7). The direction of these relationships (sign of the correlation coefficient) of carbonate system parameters with temperature and salinity at our site at the Aransas Ship Channel was the same as in open ocean waters despite these relationships not being consistent across different estuarine environments (N. Rosenau, personal communications). The strong correlations with temperature support our findings that thermal controls on pCO_2 can be important over multiple time scales. Significantly warmer water temperatures were observed during the nighttime in both summer and fall (Table 2, Fig. 8), indicating that temperature could exert a slight control on the carbonate system over a diel time scale. More substantial temperature swings between seasons indicate that temperature is more important over seasonal time scales (Table S1). In addition to direct thermal control at our site, the strong correlations with temperature are likely derived from changes in net community metabolism associated with temperature (Caffrey, 2004). For example, the strong negative correlation between nonthermal pCO_2 and temperature (Table 6S4) is likely indicative of enhanced primary productivity in warmer waters.

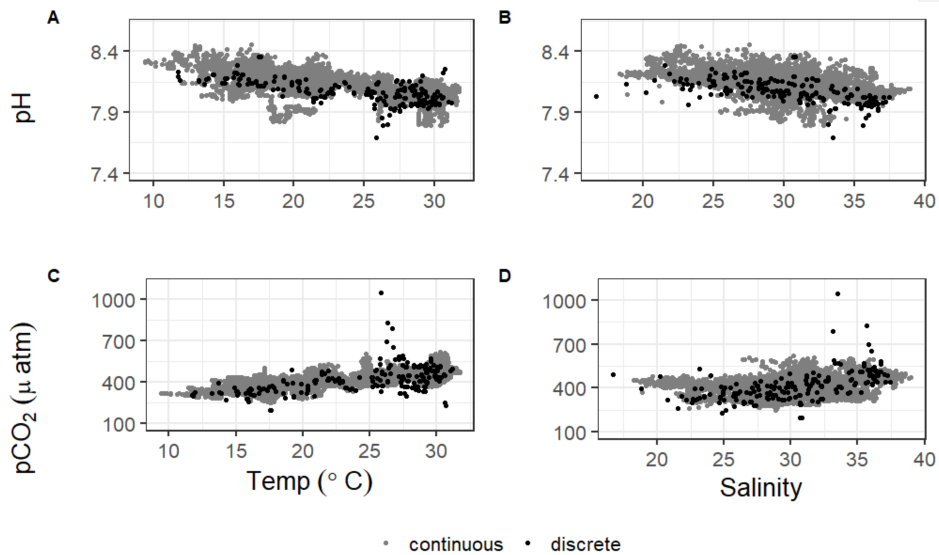

Figure 75. Correlations of pH and pCO_2 with temperature and salinity from continuous sensor data (gray) and all discrete data (black).

Table 6. Pearson correlation coefficients between surface water carbonate system parameters and other water quality and environmental parameters for both continuous sensor data and discrete sample data (entire sampling period). Only observations without significant stratification in the water column were included in these analyses. Parameter pairs with a significant correlation based on $\alpha=0.05$ have a correlation coefficient reported. Asterixis are used to indicate the level of significance of the correlation, * $p<0.05$, ** $p<0.01$, *** $p<0.0001$. The correlation coefficient is listed as 0 if the relationship was not significant. N/A is listed when the analysis was omitted because the environmental parameter did not have observations corresponding to the date and time of at least half of our discrete sample measurements (45 observations).

	pH		**pCO_2**		**pCO_2, nonthermal**	
	Continuous	**Discrete**	**Continuous**	**Discrete**	**Continuous**	**Discrete**
Temperature (°C)	-0.55 ***	-0.59 ***	0.75 ***	0.53 ***	-0.73 ***	-0.45 ***
Salinity	-0.47 ***	-0.74 ***	0.53 ***	0.69 ***	-0.28 ***	0.35 **
Wind Speed (m s^{-1})	-0.04 **	N/A	0.15 ***	N/A	0	N/A
Dissolved Oxygen (mg L^{-1})	0.55 ***	0	-0.81 ***	0	0.45 ***	0
Tide Level (m)	0	0	-0.15 ***	0	-0.15 ***	-0.55 **
Turbidity	-0.08 ***	N/A	-0.14 ***	N/A	-0.28 ***	N/A
Fluor. Chlorophyll	0.12 ***	N/A	-0.22 ***	N/A	0.34 ***	N/A

Though annual average pCO_2 and CO_2 flux are higher in the upper estuary and lower offshore than at our study site, the same seasonal pattern of elevated pCO_2 and positive

Formatted: Indent: First line: 0"

CO_2 flux in the summer and depressed pCO_2 and negative CO_2 flux during the winter observed at our site has also been observed throughout the entire MAE and in the open Gulf of Mexico (Hu et al., 2018; Yao and Hu, 2017). Seasonal fluctuations in pH and pCO_2 are low at our study site relative to other systems that have been studied to date (Carstensen et al., 2018; Yao and Hu, 2017), which may be in part due to the relatively small seasonal temperature changes (Table 1) in this warm, semiarid environment. Despite substantial seasonal thermal control at our site, simple linear regressions indicate that temperature had substantially higher explanatory value for pH and pCO_2 in offshore GOM waters (R^2 = 0.81 and 0.78, respectively (Hu et al., 2018)) than at our site (R^2 = 0.30 and 0.52, respectively, for sensor data and R^2 = 0.38 and 0.25, respectively, for discrete data).

Other physical factors that may exert control on the carbonate system (including windspeed, salinity, tide level, and turbidity) can also be investigated through parameter relationships. We investigated wind speed as a possible control on the carbonate system to gain insight into the effect of wind-driven CO_2 fluxes on the inventory of CO_2 in the water column (and subsequent impacts to the entire carbonate system). The Texas coast has relatively high wind speeds, with the mean wind speed observed during our continuous monitoring period being 5.8 m s^{-1}. While this results in relatively high calculated CO_2 fluxes (Fig. 5), the seasonal relationship between pCO_2 and windspeed does not support a change in inventory with higher winds. Linear regression analysis within each season reveals that winter, spring, and fall all experience increases in pCO_2 with increasing wind, while there is not a significant relationship in summer. Since spring and summer both have a mean estuarine pCO_2 greater than atmospheric level (and

~~positive CO_2 flux, Table 1) a negative relationship between windspeed and pCO_2 would be necessary to support this hypothesis. Linear regression analysis within each season reveals that winter, spring, and fall all experience increases in pCO_2 with increasing wind, while there is not a significant relationship in summer.~~

Previous studies have indicated that freshwater inflow may exert a primary control on the carbonate system in the estuaries of the northwestern GOM (Hu et al., 2015; Yao et al., 2020; Yao and Hu, 2017). Carbonate system variability is much lower at ASC than it is in the more upper reaches of MAE, likely due to the lesser influence of freshwater inflow and its associated changes in biological activity at ASC (Yao and Hu, 2017). ~~Increased freshwater inflow resulting from storms has also been shown to increase community respiration, which would subsequently increase pCO_2, in the upper reaches of the MAE (Bruesewitz et al., 2013). MAE is also known to experience large swings in the chemistry of its freshwater inputs, with relatively high levels of dissolved inorganic carbon and total alkalinity during base flows but much lower levels due to dilution during intense flooding (Yao et al., 2020).~~ Given the location of our sampling in the lower portion of the estuary and the long residence time in the system, we ~~will~~ did not directly address ~~freshwater inflows~~river discharge as a controlling factor, but the influence of freshwater inflow may be evident in the response of the system to changes in salinity. Fluctuating salinity at ASC may also result from direct precipitation, stratification, and tidal fluctuations; however, the low R^2 (0.02) associated with a simple linear regression between tide level and salinity ($p<0.0001$) indicates that salinity fluctuations are more indicative of non-tidal factors. ~~Carbonate system variability is much lower at our study site than it is in the more~~

Formatted: Not Highlight

Formatted: Not Highlight

Formatted: Not Highlight

Formatted: Not Highlight

Formatted: Not Highlight

upper reaches of MAE, likely due to the lesser influence of freshwater inflow and its associated changes in biological activity at the Aransas Ship Channel (Yao and Hu, 2017). Salinity data from both sensor and discrete monitoring was were strongly correlated with both pH and pCO_2, with correlation coefficients nearing (continuous) or surpassing (discrete) that of the correlations with temperature (Fig. 767; Table 6S45). Periods of lower salinity had higher pH and lower pCO_2, likely due to enhanced freshwater influence and subsequent elevated primary productivity at the study site. Fluctuating salinity at the Aransas Ship Channel may also result from direct precipitation, stratification, and tidal fluctuations. ; however, the low R^2 (0.02) associated with a simple linear regression between tide level and salinity ($p<0.0001$) indicates that salinity fluctuations are more indicative of non-tidal factors. Based on the simple linear regression of salinity with tide level, there is a significant ($p<0.0001$) relationship between tide level and salinity, but the amount of variability in salinity that tides can explain (based on model R^2) is only about 2%.

Tidal fluctuations were clearly important to carbonate system variability at the Aransas Ship Channel (Table 5). While the northwestern GOM estuaries are generally microtidal, the constricted tidal inlets such as the Aransas Ship Channel may experience relatively large tidal fluctuations. The water level data used in this analysis came from a location directly offshore from our study site, and water level had a range of 1.30 m (maximum – minimum recorded water level) over the 10-month continuous monitoring period. Mean water level varied between all seasons; mean spring (highest) water levels were on average 0.08 m higher than winter (lowest) water levels (ANOVA $p<0.0001$, fall

Formatted: Not Highlight

Formatted: Not Highlight

Formatted: Not Highlight

Formatted: Not Highlight

Formatted: Not Highlight

was not considered because of a lack of water level data). Tidal influence on pH was less clear. Data from continuous monitoring did not show a significant correlation between pH and tide level across the entire monitoring period (Table 6). Significant differences in mean pH between tide levels were recorded during each season; pH was higher at high tide (corresponding with the lower pCO_2) during the winter and summer, but pH was lower at high tide (conflicting with the lower pCO_2) in the spring (Table 5). This separation between water level correlation with pH and pCO_2 suggests that different controlling factors of the carbonate system may not be exerted equally on both pCO_2 and pH over different timescales. Similar to pH, both temperature and salinity experienced seasonally dependent reversals in their difference between tide levels during the spring; each were higher at low tide during winter and summer and higher at high tide during spring (Table 5). Given the negative relationship of both temperature and salinity with pH, it is likely these parameters became important controls on pH in the spring.

To help examine controls on the carbonate system on a diel time scale, we used loess models (locally weighted polynomial regression) to identify changes in diel patterns over the course of our monitoring period (Fig. 8). Both tidal and biological controls on the carbonate system can operate on a diel time scale. The GOM is one of the few places in the world that experiences diurnal tides (Seim et al., 1987; Thurman, 1994), so theoretically, the fluctuations in pCO_2 associated with tides may align to either amplify or reduce/reverse the fluctuations that would result from diel variability in net community metabolism. The mean daily tidal fluctuation during our continuous monitoring period was 0.39 m ± 0.13 m, which did not significantly differ between seasons (ANOVA $p=0.739$). However, diel patterns in tidal fluctuations exhibited a strong seasonal pattern during the continuous monitoring period, with spring and summer having higher tide level during the daytime and winter having higher tide level during the nighttime (Fig. 8). This same seasonal pattern in diel tidal fluctuations is exhibited from Dec 20, 2016 (when the tide data is first available) through the rest of our discrete monitoring period (Feb 25, 2020), indicating that tidal control on diel variability of carbonate system parameters was likely consistent throughout this time period.

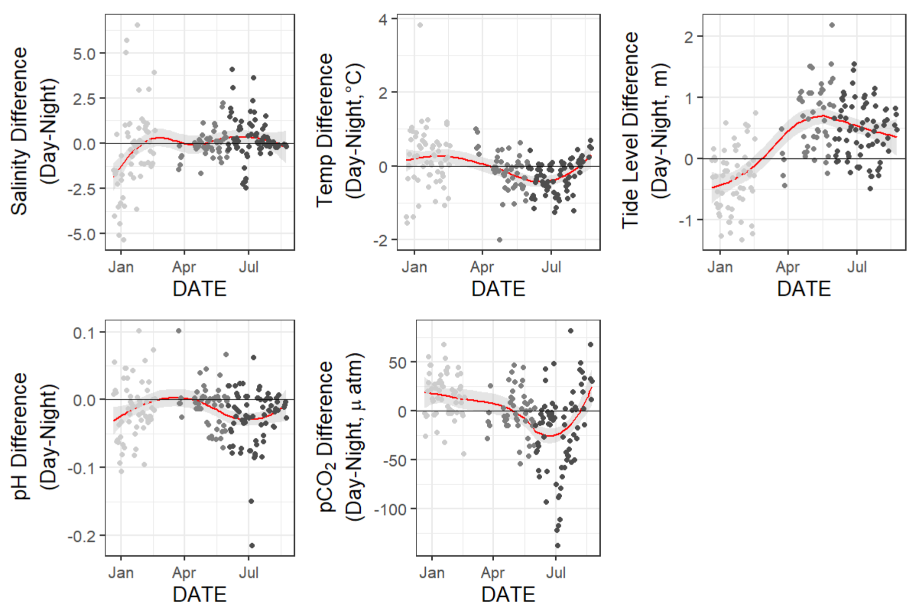

Figure 86. Loess models (red line) and their confidence intervals (gray band around red lines) showing the difference in daily parameter mean daytime minus nighttime measurements. The gray scale of the data points represents the four seasons over which data were collected.

Based on diel tidal fluctuations at this site, tidal control should amplify the biological control signal (nighttime pCO_2 > daytime pCO_2) during spring and summer and reduce or reverse the biological control signal during the winter. This was supported by our pCO_2 data, which showed nighttime pCO_2 significantly greater than daytime pCO_2 in the

Formatted: Not Highlight

Formatted: Indent: First line: 0"

summer (Table 2). The full reversal of the biological signal in the winter (Table 2, nighttime pCO_2 $<$ daytime pCO_2) indicated that biological activity was not the strongest controlling factor on the diel time scale and was likely exceeded by tidal control. Winter also had higher daytime temperature (Table 3), which could also contribute to the higher daytime pCO_2, while summer diel temperature and tides would act to amplify the biological signal.

Again, the diel variability in pH did not mirror pCO_2 as would be expected. The loess models show that daily variability in pH closely mirrors that of temperature while the daily variability in pCO_2 much closer reflects the tide level (Fig. 8), indicating that controlling factors of the carbonate system may not be exerted equally on both pH and pCO_2.

The extent of biological control on the system can also be investigated based on correlations between carbonate system parameters and dissolved oxygen (DO). Respiration-driven acidification is one of the most important local to regional contributors to acidification in coastal waters, with acidification closely linked to the widespread issue of deoxygenation (Rabalais et al., 2014; Strong et al., 2014). There were no observations of hypoxia at our study site during our monitoring, with minimum DO levels of 3.9 mg L^{-1} and 4.0 mg L^{-1} for our continuous monitoring period and our discrete sampling period, respectively. Despite the lack of hypoxia, there was a strong relationship between the carbonate system parameters and DO (Table 6), suggesting that net ecosystem metabolism may exert an important control on the carbonate system on certain time scales.

There was no significant difference in daytime and nighttime DO during any season (paired t-tests, winter p = 0.1573, spring p = 0.4877, summer p = 0.794) The lack of difference between daytime and nighttime DO despite the significant differences in pH and pCO_2 between daytime and nighttime (Table 2). This suggests that net community metabolism is likely not a strong controlling factor of carbonate system parameters at this site on a diel time scale. The control exerted on the carbonate system by biological processes is likely much greater on the seasonal scale than the diel scale. The correlation between continuous pCO_2 and DO is stronger than pCO_2 and temperature, which suggests strong biological control and supports the indication by T/B values that non-thermal processes exert more control on pCO_2 than temperature. Both types of sampling (i.e., continuous and discrete) demonstrate that pH is generally highest in the winter and lowest in the summer and pCO_2 is highest in the summer and lowest in the winter (Figs. 2, and 3, Table 1). Though this seasonal pattern corresponds with the directional response from temperature fluctuations, it can also be explained by biological activity. We investigated wind speed as a possible control on the carbonate system to gain insight into the effect of wind-driven CO_2 fluxes on the inventory of CO_2 in the water column (and subsequent impacts to the entire carbonate system). The Texas coast has relatively high wind speeds, with the mean wind speed observed during our continuous monitoring period being 5.8 m s^{-1}. While this results in relatively high calculated CO_2 fluxes (Fig. 3), the seasonal relationship between pCO_2 and windspeed does not support a change in inventory with higher winds. Since spring and summer both have a mean estuarine pCO_2 greater than atmospheric level (and positive CO_2 flux, Table S1) a negative relationship between windspeed and pCO_2 would be necessary to support this hypothesis, but winter,

Formatted: Not Highlight

spring, and fall all experience increases in $p$$CO_2$ with increasing wind based on simple linear regression.

Given that this sampling location is in a ship channel where boat traffic (including large oil tankers) is relatively heavy, there is potential for atmospheric deposition of acids (SOx and NOx) to play a role in the carbonate system variability (Doney et al. 2007, Hunter et al. 2011). To try to understand this control, we deployed air samplers at our study site for eight 2-week periods. The levels of atmospheric NO_2 and SO_2 did not vary widely over the time period. NO_2 was ranged 5.45 to 6.99 ppb (6.13 ± 0.63 ppb), and SO_2 ranged 1.15 to 1.18 ppb (1.43 ± 0.35 ppb) over the sampling dates (J. D. Felix, personal communications). There was no apparent correlation between these values and the pH or $p$$CO_2$ levels over the 2-week sampling periods.

Co-locating our pH and $p$$CO_2$ sensors with other coastal environmental monitoring sensors allowed insight into correlated environmental parameters and potential driving forces of carbonate chemistry on diel and seasonal time scales. The results of this study provide strong support for the continued implementation of carbonate chemistry monitoring in conjunction with preexisting coastal environmental monitoring infrastructure. Our understanding of any estuarine system could benefit from long-term effective deployments of these monitoring tools. Strategically locating carbonate chemistry sensors at estuarine sites that are subject to local OA drivers or support large biodiversity or commercially important species may be the most crucial in guiding future mitigation and adaptation strategies for natural systems and aquaculture facilities (Chan et al., 2013; Strong et al., 2014).

4.32 Carbonate chemistry as a component of overall estuarine system variability

Estuaries and coastal areas are dynamic systems with human influence, riverine influence, and influence from an array of biogeochemical processes, resulting in highly variable chemical and eenvironmental conditions. Based on an LDA used to assess overall system variability using a suite of environmental parameters compiled at a single location, we can conclude that carbonate chemistry parameters are among the most important of variants on both daily and seasonal time scales in this coastal setting. Of the two carbonate system components that we incorporated (pH and pCO_2), pCO_2 was the most critical in discriminating along diel or seasonal scales, despite similar seasonal differences that were identified by ANOVA (Table S2) and more seasons with significant diel differences in pH (Table S3). pH seemed to be a larger component of overall system variability on a seasonal time scale (compared to the very small contribution seen on a diel scale, Table 1). Given that the seasonal and diel variability in carbonate chemistry at this location is relatively small compared to other coastal areas that are in the literature, the high contribution of carbonate chemistry to overall system variability that we detected is likely to be present at other coastal locations around the world.

Formatted: Font: Italic

Formatted: Subscript

Formatted: Font: Italic

Formatted: Subscript

Formatted: Not Superscript/ Subscript

The contribution of pH to discriminating along diel or seasonal scales was less than pCO_2 despite the same seasonal differences that were identified by ANOVA (Table 3) and more seasons with significant diel differences (Table 2). However, pH still seemed to be relatively important on seasonal scales, having clearer contribution to seasonal system variability than several other parameters including DO and salinity.

To better understand overall system variability over different time scales, we used a linear discriminant (LD) analysis, a multivariate statistic that allows dimensional reduction, to determine the linear combination of environmental parameters (individual parameters reduced into linear discriminants, LDs) that allow the best differentiation between day and night as well as between seasons. This used the same suite of environmental data and data sources as Sect. 4.1.2.

All variables were centered and scaled to allow direct comparison of their contribution to the system variability. The magnitude (absolute value) of coefficients of the LDs (Table 7) represents the relative importance of each individual environmental parameter in the best discrimination between day and night and between seasons, i.e., the greater the absolute value of the coefficient, the more information the associated parameter can provide about whether the sample came from day or night (or winter, spring, or summer). Only one LD could be created for the diel variability (since there are only two classes to discriminate between – day and night). Two LDs could be created for the seasonal variability (since there were three classes to discriminate between – fall was omitted because of the lack of tidal data), but only the coefficients for LD1 are reported (Table 7) given that LD1 captured 95.64% of the seasonal variability.

Table 73. Coefficients of linear discriminants (LD) from discriminant function analysis (DFA) using continuous sensor data and other environmental parameters. Results for discriminants for both diel and seasonal variability shown. All variables were centered and scaled. For the seasonal analysis, only LD1 is given since it was captured 95.64% of the variability (for the diel analysis, there is only one . Given that many of the water quality parameters were measured in bottom waters and our sensors were measuring surface waters, only those observations without significant stratification in the water column (a salinity difference of less than 3 between surface and bottom) were included in these analyses.

	Diel	Seasonal
	LD1	LD1
Temperature (°C)	0.5406	-3.5279
Salinity	0.1473	0.0432

Formatted: Indent: First line: 0.5"

pCO_2 (µatm)	-0.1612	-0.2928
pH	0.0593	0.0991
Tide Level (m)	0.0968	-0.2389
Wind speed (ms^{-1})	-0.0009	0.0504
Total PAR	-2.2878	-0.0676
DO (mg L^{-1})	-0.0839	0.0859
Turbidity	-0.0561	0.1455
Fluor. Chlorophyll	0.1397	-0.4040

As would be expected, we found that PAR provided the most differentiation between daytime and nighttime conditions (based on the largest coefficient associated with Diel LD1, Table 7). Temperature was the second most important factor in differentiating between day and night; this corresponds to the diel variability that we detected where both summer and fall had clear separation of mean temperature between day and night, with nighttime temperatures being 0.3 and 1.0 higher, respectively (Table 3). The next most important parameter in differentiating between day and night in this system was pCO_2, providing more evidence for differentiation between day and night than other parameters that would be expected to vary on a diel timescale (e.g. chlorophyll and DO). As for system variability that allowed differentiation between the four seasons, the most important parameter in system variability was temperature (Table 7, Seasonal LD1), as would be expected with the clear seasonal temperature fluctuations (Fig. 2E). The second most important parameter in contributing to seasonal variability was chlorophyll, likely indicating clear seasonal blooms. The third most important parameter for seasonal differentiation was pCO_2; therefore pCO_2 variability seems to be more closely tied to seasons than variability in tide level, DO, or the array of other parameters (Table 7).

The contribution of pH to discriminating along diel or seasonal scales was less than pCO_2 despite the same seasonal differences that were identified by ANOVA (Table 3) and

Formatted: Indent: First line: 0"

more seasons with significant diel differences (Table 2). However, pH still seemed to be relatively important on seasonal scales, having clearer contribution to seasonal system variability than several other parameters including DO and salinity.

We can conclude that carbonate chemistry parameters are among the most important of variants on both daily and seasonal time scales in this coastal setting. Compared to six other estuaries around the United States with similar sensor deployments for carbonate chemistry characterization, our study site has a relatively small range of pH and pCO_2 on both diel and seasonal scales (N. Rosenau, personal communication). While we do not have the same suite of environmental data for these other systems, this suggests that the relative amount of system variability contributed by carbonate chemistry may be even greater in other estuarine systems. The relatively small fluctuations in pH and pCO_2 that are seen on a daily scale at the Aransas Ship Channel is likely due to the subtropical setting with little ocean upwelling influence and the lower estuary position of our monitoring (further removed from the already small freshwater influence), but it may also be tied to the system's relatively high buffer capacity. Just as the extent of hypoxia-induced acidification was relatively low in Corpus Christi Bay compared to other systems because of the bay's high buffer capacity (McCutcheon et al., 2019), the extent of pH fluctuation on a daily scale from biological activity would also be modulated by the intrinsic buffer capacity, which is likely also high in this system due to high alkalinity in the freshwater endmembers (Yao et al., 2020).

4.3 Comparing continuous monitoring and discrete sampling

4.3.1 Representative sampling in a temporally variable environment

Commented [m3]: Moved from results:
; this corresponds to the diel variability that we detected where both summer and fall had clear separation of mean temperature between day and night, with nighttime temperatures being 0.3 and 1.0 higher, respectively (Table 3).

~~Discrete water sample collection and analysis is the most common method that has been employed to attempt to understand the carbonate system of estuaries. However, it is difficult to know if these samples are representative of the spatial and temporal variability in carbonate system parameters. While this time-series study cannot conclude whether our broader sampling efforts in the MAE are representative of the spatial variability in the estuary, it can investigate how representative our bimonthly to monthly sampling is of the more high-frequency temporal variability that the Aransas Ship Channel experiences.~~

~~One-way ANOVAs were conducted to compare between monitoring methods (separate one-way ANOVAs within each season because of the significant interaction between these factors in an initial two-way ANOVA). There were three levels of monitoring method included in the comparison of means: continuous monitoring, discrete monitoring during only the continuous monitoring period, and discrete monitoring over the entire period (C, D_C, and D, respectively, in Table 3). To interpret the results, a difference in means between the continuous monitoring and discrete monitoring datasets would only indicate that the 10-month period of continuous monitoring was not representative of the 5+ year period that discrete samples have been collected, but a difference in means between the continuous data and discrete sample data collected during the continuous monitoring period represents discrepancies between types of monitoring.~~

~~There were several instances where seasonal parameter means significantly differed between the 10-month continuous monitoring period and the 5+ year discrete sampling period (Table 3, $C \neq D$ or $D_c \neq D$) including temperature in the summer and~~

fall, salinity in the spring, pH in the summer and fall, and pCO_2 in winter, spring, and summer. While clear seasonal variability was demonstrated for most parameters (using both continuous and discrete data for the entire period), these differences between the 10-month continuous monitoring period and our 5+ year monitoring period illustrate that there is also interannual variability in the system. Therefore, short periods of monitoring are unable to fully capture current baseline conditions.

During the continuous monitoring period (2016-2017), we found no significant difference between sampling methods in the seasonal mean temperature, salinity, or pCO_2. The two sampling methods also resulted in the same mean pH for all seasons except for summer, when the sensor data recorded a higher mean pH than discrete samples (Tables 1 and 3). During this case, we can conclude that discrete monitoring did not accurately represent the system variability that was able to be captured by the sensor monitoring. However, given that most seasons did not show differences in pH or pCO_2 between sampling methods, the descriptive statistics associated with the discrete monitoring did a fair job of representing system means. This is evidence that long-term discrete monitoring efforts, which are much more widespread in estuarine systems than sensor deployments, can be generally representative of the system despite known temporal variability on shorter time scales.

Understanding the relationships of pH and pCO_2 with temperature and salinity is important in a system. Both the continuous and discrete sampling types indicate that pH has a significant negative relationship with both temperature and salinity and pCO_2 has a s significant positive relationship with both temperature and salinity (Fig. 7). Based on the results of an Analysis of Covariance (ANCOVA), the relationship (slope) of pH with both temperature and salinity and of pCO_2 with salinity were not significantly different between types of monitoring (considering the sensor deployment period only), supporting the effectiveness of long-term discrete monitoring programs when sensors are unable to be deployed. However, ANCOVA did reveal the relationship of pCO_2 with temperature is significantly different (method:temp $p=0.0062$) between monitoring methods.

While *in situ*continuous monitoring data from sensors is usually lacking good substantial spatial coverage, it is effective in capturing temporal resolution and presumably providing better estimates of average CO_2 flux at a given location versus periodic sampling. Previous studies have pointed out that discrete sampling methods, which generally involve only daytime sampling, do not adequately capture the diel variability in the carbonate system and may therefore lead to underestimation of CO_2 fluxes. However, we found no significant difference (within any season) between CO_2 flux values calculated with sensor data versus discrete samples (Table 3). Calculated CO_2 fluxes also did not significantly differ between day and night during any season, despite some differences in pCO_2 (Table 2), likely due to the large error associated with the calculation of CO_2 flux (Table 1, Fig. 5) which will be further discussed below. Therefore, the expected underestimation of CO_2 flux based on diel variability of pCO_2 was not encountered at our study site, validating the use of discrete samples for quantification of CO_2 fluxes (until methods with less associated error are available). Even given less error in calculated flux, estimated fluxes would likely not differ between methods on an annual scale (as pCO_2 did not), but CO_2 fluxes may differ on a seasonal scale since the differences between daytime and nighttime pCO_2 were not consistent across seasons (Table 2).

There are many factors contributing to error associated with CO_2 flux. There is still large error associated with estimates of estuarine CO_2 flux because turbulent mixing is difficult to model and turbulence is the main control on CO_2 gas transfer velocity, *k*, in shallow water environments. Thus, our wind speed parameterization of *k* is imperfect and likely the greatest source of error. Other notable sources of error include the data treatment. For example, we chose to seasonally weight the individual calculated flux values in the calculation of annual flux to account for differences in sampling frequency between seasons. From continuous data, the weighted average flux was 0.2 mmol m^{-2} d^{-1}, although choosing not to seasonally weight and simply look at the arithmetic mean of fluxes calculated directly from sampling dates would have resulted in an annual CO_2 flux of -0.7 mmol m^{-2} d^{-1} for the same period. Similarly, the weighted average flux from all 5+ years of discrete data was -0.9 mmol m^{-2} d^{-1}, but the arithmetic mean of fluxes would have resulted in an annual CO_2 flux of 0.2 mmol m^{-2} d^{-1} for the same period. Another source of error that could be associated with the calculation of flux from the discrete data is the way in which wind speed data are aggregated to be used in the windspeed parameterization. We decided to use daily averages of the windspeed for calculations. Using the windspeed measured for the closest time to our sampling time or the monthly averaged wind speed may have resulted in very different flux values.

4.3.2 Direct agreement of measurement methods and quantified uncertainties associated with parameters

Direct comparisons were made between measurements from sensors and laboratory-analyzed bottle samples – including both quality control (QC) samples taken from the cooler that housed the sensors at the time when these sensors took recorded readings and long-term monitoring samples taken from the ship channel near the sensors (within 100 m) that occurred at various times and were compared to sensor measurements of the closest full hour (Table 8). The mean difference between the SeaFET pH measurements and the QC samples (continuous – discrete) prior to sensor data correction was 0.05 ± 0.08 (Table 8, which would reduce to 0.00 ± 0.08 following the correction). The mean difference between the SAMICO2 pCO_2 measurements and the QC samples (continuous – discrete) was -18 ± 44 (Table 8) when discrete sample pCO_2 was calculated using Millero (2010) constants. We used several different constants to calculate pCO_2 to check this offset; all were similar in mean and standard deviation, but the offset could be slightly reduced using Millero (2002) constants.

Table 84. Comparison of discrete and continuous monitoring. The difference between sampling methods is reported in two different ways: the difference between sensor measurements and laboratory measurement of quality control (QC) bottle samples taken directly from the cooler (here the pH difference is prior to the sensor pH correction of +0.05), and the difference between sensor measurements and laboratory measurement of bottle samples taken from a nearby station for our 5+ year monitoring (here the pH difference if after the sensor pH correction of +0.05, see methods for details). For all calculated parameters, dissociation constants from Millero 2010 were used. Error – analytical error for directly measured parameters and propagated error for calculated parameters (mean ± standard deviation, calculated in the seacarb package in R) associated with carbonate system variables is also reported.

	Difference between sampling methods (mean difference ± standard deviation of the difference)		**Error (Analytical or Propagated)**	
	Sensor – QC cooler samples (prior to sensor pH correction, n=12)	Sensor – discrete samples (after pH sensor correction, n=13)	**Discrete Sampling (n = 104)**	**Continuous Monitoring (n = 6088)**
Temperature (°C)			0.1	0.1
Salinity	-0.16 ± 1.44	0.50 ± 1.69	0.01	0.1
pH	-0.05 ± 0.08	0.01 ± 0.12	0.0004	0.05
pCO_2 (µatm)	-18 ± 44	25 ± 63	7 ± 2	1.0
DIC (µmol kg^{-1})			±2.5	327.4 ± 63.2
TA (µmol kg^{-1})			7.4 ± 0.9	400.7 ± 81.0
Ω_{Ar}			0.19 ± 0.03	1.08 ± 0.31

Formatted Table

Given that the analytical accuracy of the SeaFET instrument is 0.05 pH units, the average offset between sensor and laboratory values of quality control samples demonstrates fair agreement (Table 8). Given that calculated uncertainty associated with calculated discrete pCO_2 was 7 ± 2, we did not see great agreement between SAMICO2 pCO_2 and laboratory-calculated pCO_2 for quality control samples (mean difference of -18 ± 44, Table 8). Mean offsets and their associated standard deviations were larger when comparing sensor data to samples taken during our long-term discrete monitoring effort. This is not surprising given that the discrete sample collection did not occur at the exact time of the sensor measurement or the exact location of the cooler pump inlet. Greater sensor-laboratory agreement has been achieved for open ocean settings, but this larger standard deviation is likely a result of the temporal variability in the more complex estuarine environment where these instruments have been much less widely deployed to date.

Propagation of error associated with computed carbonate system parameters was done using the *seacarb* package in R (Gattuso et al., 2018); the error propagation includes error associated with the measurements of the input pair (1 µatm for pCO_2 from SAMICO2 and 0.05 for pH from SeaFET; 0.0004 for laboratory spectrophotometric pH and 2.5 µmol kg^{-1} for laboratory DIC), error associated with *in situ* temperature (0.1 °C) and salinity (0.1 for sensor-measured and 0.01 for laboratory-measured), and error associated with total boron the key dissociation constants (standard recommended error used) (Table 8). While the error associated with calculated parameters from discrete bottle samples was relatively small and likely a result of uncertainties in constants (Orr et al., 2018), we note that the error associated with the calculated dissolved inorganic carbon (DIC), total alkalinity (TA), and saturation state of aragonite (Ω_{Ar}), which are other frequently addressed carbonate system parameters, from sensor data was relatively large when calculated with sensor data(Table 8). This large error is likely a result of both the relatively low analytical precision associated with the pH sensor and the poor mathematical combination of variables for speciation calculations. Hence, we limited the discussion to pH (which was directly measured for both continuous monitoring and laboratory analysis of discrete samples) and pCO_2 (which was directly measured for continuous monitoring and had relatively low error when calculated with discrete sample DIC and pH, Table 8) and omitted any discussion of the parameters with high propagation error. The high error suggests that it may be important to develop and broadly use autonomous sensors that can measure carbonate system parameters that allow for lower propagated error to have a full picture of estuarine carbonate chemistry on high-frequency time scales.

5. Conclusions

We monitored carbonate chemistry parameters (pH and pCO_2) using both sensor deployments (10 months) and discrete sample collection (5+ years) at the Aransas Ship Channel, TX, to characterize temporal variability and investigate controlling factors. Significant seasonal variability and diel variability in carbonate system parameters were both present at the location. Carbonate chemistry parameters were among the most important environmental parameters to distinguish between both diel and seasonal environmental conditions.

Diel fluctuations were smaller than many other areas previously studied. The difference between daytime and nighttime values of carbonate system parameters varied between seasons, occasionally reversing the expected diel variability due to biological processes. Tide level (despite the small tidal range), temperature, freshwater influence, and biological activity ~~, and tide level (despite the small tidal range)~~ all seem to exert important controls on the carbonate system at the location. The relative importance of the different controls varied with timescale, and controls were not always exerted equally on both pH and pCO_2. Carbonate chemistry (particularly pCO_2) was among the most important environmental parameters to in overall system variability to distinguish between both diel and seasonal environmental conditions.

Despite known temporal variability on shorter timescales, discrete sampling was generally representative of the average carbonate system on a seasonal and annual basis based on comparison with our sensor data. Additionally, there was no difference in CO_2 flux between sampling types, supporting the validity of discrete sample collection for carbonate system characterization at this location.

Formatted: Indent: First line: 0.5"

This is one of the first studies that investigates high-temporal frequency data from deployed sensors that measure carbonate system parameters in an estuary-influenced environment. Long-term, effective deployments of these monitoring tools could greatly improve our understanding of estuarine systems. This study's detailed investigation of data from multiple, co-located environmental sensors was able to provide insight into potential driving forces of carbonate chemistry on diel and seasonal time scales; this provides strong support for the implementation of carbonate chemistry monitoring in conjunction with preexisting coastal environmental monitoring infrastructure, which has had little application in estuarine environments thus far. Strategically locating such sensors in areas that are subject to local OAacidification drivers or support large biodiversity or commercially important species may be the most crucial in guiding future mitigation and adaptation strategies for natural systems and aquaculture facilities.Both sampling methods demonstrated significant seasonal variability at the location, with highest pH (lowest pCO_2) in the winter and lowest pH (highest pCO_2) in the summer. Significant diel variability was also evident from sensor data, though diel fluctuations were smaller than many other areas previously studied.The difference between daytime and nighttime values of carbonate system parameters varied between seasons, occasionally reversing the expected diel variability due to biological processes.

Carbonate chemistry parameters were among the most important environmental parameters to distinguish between both diel and seasonal environmental conditions. The difference between daytime and nighttime values of carbonate system parameters varied between seasons, occasionally reversing the expected diel variability due to biological processes. It was evident that biological activity is not the strongest controlling factor of diel variability at this location, likely surpassed by tidal control despite the small tidal range in the northwestern GOM. Controls on the system also differed over different time scales, with temperature becoming a less important control over shorter time scales. Tides exerted significant control on the carbonate system, and low tide allowed more biological control of the system. Higher mean pCO_2 was reported for low tide versus high tide across all seasons. pH was higher at high tide during winter and summer but deviated from the expected pattern during spring with lower pH during high tide. The results

Formatted: Indent: First line: 0"

suggest that the controlling factors of the carbonate system may not be exerted equally on both pH and pCO_2 on diel timescales, causing separation of their diel or tidal relationships during certain seasons. The detailed investigation of controlling factors provides strong support for the implementation of carbonate chemistry monitoring in conjunction with preexisting coastal environmental monitoring infrastructure, which has had little application in estuarine environments thus far.

Despite known temporal variability on shorter timescales, discrete sampling was generally representative of the average carbonate system on a seasonal and annual basis based on comparison with our sensor data. Additionally, there was no difference in CO_2 flux between sampling types supporting the validity of discrete sample collection for carbonate system characterization. Co-locating our pH and pCO_2 sensors with other coastal environmental monitoring sensors allowed insight into correlated environmental parameters and potential driving forces of carbonate chemistry on diel and seasonal time scales. The results of this study provide strong support for the continued implementation of carbonate chemistry monitoring in conjunction with preexisting coastal environmental monitoring infrastructure. Our understanding of any estuarine system could benefit from long-term effective deployments of these monitoring tools. Strategically locating carbonate chemistry sensors at estuarine sites that are subject to local OA drivers or support large biodiversity or commercially important species may be the most crucial in guiding future mitigation and adaptation strategies for natural systems and aquaculture facilities (Chan et al., 2013; Strong et al., 2014).

Formatted: Indent: First line: 0"

Data availability

Continuous sensor data are archived with the National Oceanic and Atmospheric Administration's (NOAA's) National Centers for Environmental Information (NCEI) (https://doi.org/10.25921/dkg3-1989). Discrete sample data are available in two separate datasets archived with National Science Foundation's Biological & Chemical Oceanography Data Management Office (BCO-DMO) (doi:10.1575/1912/bco-dmo.784673.1 and doi: 10.26008/1912/bco-dmo.835227.1).

Author Contribution

MM and XH defined the scope of this work. XH received funding for all components of the work. MM, HY, and CJS performed field sampling and laboratory analysis of samples. MM prepared the initial manuscript and all co-authors contributed to revisions.

Competing interests

The authors declare that they have no conflict of interest.

Formatted: Font: (Default) Times New Roman

Acknowledgements

Funding for autonomous sensors and sensor deployment was provided by the United States Environmental Protection Agency's National Estuary Program via the Coastal Bend Bays and Estuaries Program Contract No. 1605. Thanks to Rae Mooney from Coastal Bend Bays and Estuaries Program for assistance in the initial sensor setup. Funding for discrete sampling as well MM's dissertation research has been supported by both NOAA National Center for Coastal Ocean Science (Contract No. NA15NOS4780185) and NSF Chemical Oceanography Program (OCE-1654232). We also appreciate the support from the Mission-Aransas National Estuarine Research

Reserve in allowing us the boat-of-opportunity for our ongoing discrete sample collections and the University of Texas Marine Science Institute for allowing us access to their research pier for the sensor deployment. A special thanks to Hongjie Wang, Lisette Alcocer, Allen Dees, and Karen Alvarado for assistance with field work.

References

Barton, A., Waldbusser, G.G., Feely, R.A., Weisberg, S.B., Newton, J.A., Hales, B., Cudd, S., Eudeline, B., Langdon, C.J., Jefferds, I., King, T., Suhrbier, A., Mclaughlin, K., 2015. Impacts of ~~Coastal~~ coastal ~~Acidification~~ acidification on the ~~Pacific~~ pacific ~~Northwest~~ northwest ~~Shellfish~~ shellfish ~~Industry~~ industry and ~~Adaptation~~ adaptation ~~Strategies~~ strategies ~~Implemented~~ implemented in ~~Response~~response. Oceanography 28, 146–159.

Bednaršek, N., Tarling, G.A., Bakker, D.C.E., Fielding, S., Jones, E.M., Venables, H.J., Ward, P., Kuzirian, A., Lézé, B., Feely, R.A., Murphy, E.J., 2012. Extensive dissolution of live pteropods in the Southern Ocean. Nat. Geosci. 5, 881–885. https://doi.org/10.1038/ngeo1635

Borges, A. V., 2005. Do w~~W~~e h~~H~~ave e~~E~~nough p~~P~~ieces of the j~~J~~igsaw to i~~I~~ntegrate CO$_2$ f~~F~~luxes in the c~~C~~oastal o~~O~~cean ? Estuaries 28, 3–27.

Caffrey, J.M., 2004. Factors controlling net ecosystem metabolism in U.S. estuaries. Estuaries 27, 90–101. https://doi.org/10.1007/BF02803563

Cai, W.-J., 2011. Estuarine and c~~C~~oastal o~~O~~cean c~~C~~arbon p~~P~~aradox: CO~~-~~$_2$ s~~S~~inks or ~~S~~sites of t~~T~~errestrial c~~C~~arbon i~~I~~ncineration? Ann. Rev. Mar. Sci. 3, 123–145. https://doi.org/10.1146/annurev-marine-120709-142723

Cai, W.-J., Hu, X., Huang, W.-J., Murrell, M.C., Lehrter, J.C., Lohrenz, S.E., Chou, W.-

Formatted: Subscript

C., Zhai, W., Hollibaugh, J.T., Wang, Y., Zhao, P., Guo, X., Gundersen, K., Dai, M., Gong, G.-C., 2011. Acidification of subsurface coastal waters enhanced by eutrophication. Nat. Geosci. 4, 766–770. https://doi.org/10.1038/ngeo1297

Challener, R.C., Robbins, L.L., Mcclintock, J.B., 2016. Variability of the carbonate chemistry in a shallow, seagrass-dominated ecosystem: Implications for ocean acidification experiments. Mar. Freshw. Res. 67, 163–172. https://doi.org/10.1071/MF14219

Challener, R.C., Robbins, L.L., McClintock, J.B., 2016~~5~~. Variability of the carbonate chemistry in a shallow , seagrass-dominated ecosystem : implications for ocean acidification experiments. Mar. Freshw~~. Res~~. Res. 67, 163–172. https://doi.org/10.1071/MF14219

Crosswell, J.R., Anderson, I.C., Stanhope, J.W., Van Dam, B., Brush, M.J., Ensign, S., Piehler, M.F., McKee, B., Bost, M., Paerl, H.W., 2017. Carbon budget of a shallow, lagoonal estuary: Transformations and source-sink dynamics along the river-estuary-ocean continuum. Limnol. Oceanogr. 62, S29–S45. https://doi.org/10.1002/lno.10631

Cyronak, T., Andersson, A.J., D’Angelo, S., Bresnahan, P., Davidson, C., Griffin, A., Kindeberg, T., Pennise, J., Takeshita, Y., White, M., 2018. Short-~~Term~~ term ~~Spatial~~ spatial and ~~Temporal~~ temporal ~~Carbonate~~ carbonate ~~Chemistry~~ chemistry ~~Variability~~ variability in ~~Two~~ two ~~Contrasting~~ contrasting ~~Seagrass~~ seagrass ~~Meadows~~meadows: Implications for pH ~~Buffering~~ buffering ~~Capacities~~capacities. Estuaries and Coasts 41, 1282–1296. https://doi.org/10.1007/s12237-017-0356-5

Dickson, A.G., 1990. Standard potential of the reaction: AgCl(s) + 1 2H2(g) = Ag(s) +

HCl(aq), and and the standard acidity constant of the ion HSO4- in synthetic sea water from 273.15 to 318.15 K. J. Chem. Thermodyn. 22, 113–127. https://doi.org/10.1016/0021-9614(90)90074-Z

Ekstrom, J. a., Suatoni, L., Cooley, S.R., Pendleton, L.H., Waldbusser, G.G., Cinner, J.E., Ritter, J., Langdon, C., van Hooidonk, R., Gledhill, D., Wellman, K., Beck, M.W., Brander, L.M., Rittschof, D., Doherty, C., Edwards, P.E.T., Portela, R., 2015. Vulnerability and adaptation of US shellfisheries to ocean acidification. Nat. Clim. Chang. 5, 207–214. https://doi.org/10.1038/nclimate2508

Gattuso, J., Epitalon, J., Lavigne, H. and Orr, J. (2021). seacarb: Seawater Carbonate Chemistry. R package version 3.2.15. https://CRAN.R-project.org/package=seacarb

Gazeau, F., Quiblier, C., Jansen, J.M., Gattuso, J.-P., Middelburg, J.J., Heip, C.H.R., 2007. Impact of elevated CO 2 on shellfish calcification. Geophys. Res. Lett. 34, L07603. https://doi.org/10.1029/2006GL028554

Gobler, C.J., Talmage, S.C., 2014. Physiological response and resilience of early life-stage Eastern oysters (Crassostrea virginica) to past , present and future ocean acidification 2, 1–15. https://doi.org/10.1093/conphys/cou004.Introduction

Ho, D.T., Law, C.S., Smith, M.J., Schlosser, P., Harvey, M., Hill, P., 2006. Measurements of air-sea gas exchange at high wind speeds in the Southern Ocean : Implications for global parameterizations. Geophys. Res. Lett. 33, 1–6. https://doi.org/10.1029/2006GL026817

Hofmann, G.E., Smith, J.E., Johnson, K.S., Send, U., Levin, L. a, Micheli, F., Paytan, A., Price, N.N., Peterson, B., Takeshita, Y., Matson, P.G., Crook, E.D., Kroeker, K.J., Gambi, M.C., Rivest, E.B., Frieder, C. a, Yu, P.C., Martz, T.R., 2011. High-

Formatted: Indent: Left: 0", Hanging: 0.4", Widow/Orphan control, Adjust space between Latin and Asian text, Adjust space between Asian text and numbers, Pattern: Clear (White), Tab stops: 0.64", Left + 1.27", Left + 1.91", Left + 2.54", Left + 3.18", Left + 3.82", Left + 4.45", Left + 5.09", Left + 5.73", Left + 6.36", Left + 7", Left + 7.63", Left + 8.27", Left + 8.91", Left + 9.54", Left + 10.18", Left

Formatted: Font: Font color: Black, Check spelling and grammar, Border: : (No border)

frequency dynamics of ocean pH: a multi-ecosystem comparison. PLoS One 6, e28983. https://doi.org/10.1371/journal.pone.0028983

Hsu S. A., 1994. Determining the Power-Law Wind-Profile Exponent under Near-Neatral Stability Condidtions at Sea. J. Appl. Meteorol. 33, 757–765.

Hu, X., Beseres Pollack, J., McCutcheon, M.R., Montagna, P. a., Ouyang, Z., 2015. Long-term alkalinity decrease and acidification of estuaries in Northwestern Gulf of Mexico. Environ. Sci. Technol. 49, 3401–3409. https://doi.org/10.1021/es505945p

Hu, X., Nuttall, M.F., Wang, H., Yao, H., Staryk, C.J., McCutcheon, M.R., Eckert, R.J., Embesi, J.A., Johnston, M.A., Hickerson, E.L., Schmahl, G.P., Manzello, D., Enochs, I.C., DiMarco, S., Barbero, L., 2018. Seasonal variability of carbonate chemistry and decadal changes in waters of a marine sanctuary in the Northwestern Gulf of Mexico. Mar. Chem. 205, 16–28. https://doi.org/10.1016/j.marchem.2018.07.006

Jiang, L.-Q., Cai, W.-J., Wang, Y., 2008. A comparative study of carbon dioxide degassing in river- and marine-dominated estuaries. Limnol. Oceanogr. 53, 2603–2615. https://doi.org/10.4319/lo.2008.53.6.2603

Jiang, L.Q., Cai, W.J., Wang, Y., Bauer, J.E., 2013. Influence of terrestrial inputs on continental shelf carbon dioxide. Biogeosciences 10, 839–849. https://doi.org/10.5194/bg-10-839-2013

Kealoha, A.K., Shamberger, K.E.F., DiMarco, S.F., Thyng, K.M., Hetland, R.D., Manzello, D.P., Slowey, N.C., Enochs, I.C., 2020. Surface ~~Water~~ water CO_2 variability in the Gulf of Mexico (1996–2017). Sci. Rep. 10, 1–13. https://doi.org/10.1038/s41598-020-68924-0

Formatted: Subscript

Laruelle, G.G., Cai, W.-J., Hu, X., Gruber, N., Mackenzie, F.T., Regnier, P., 2018. Continental shelves as a variable but increasing global sink for atmospheric carbon dioxide. Nat. Commun. 9, 454. https://doi.org/10.1038/s41467-017-02738-z

Li, D., Chen, J., Ni, X., Wang, K., Zeng, D., Wang, B., Jin, H., Huang, D., Cai, W.-J., 2018. Effects of biological production and vertical mixing on sea surface pCO_2 variations in the Changjiang River plume during early autumn: A buoy-based time series study. J. Geophys. Res. Ocean. 123, 6156–6173. https://doi.org/10.1029/2017JC013740

Mathis, J.T., Pickart, R.S., Byrne, R.H., Mcneil, C.L., Moore, G.W.K., Juranek, L.W., Liu, X., Ma, J., Easley, R.A., Elliot, M.M., Cross, J.N., Reisdorph, S.C., Bahr, F., Morison, J., Lichendorf, T., Feely, R.A., 2012. Storm-induced upwelling of high pCO_2 waters onto the continental shelf of the western Arctic Ocean and implications for carbonate mineral saturation states 39, 4–9. https://doi.org/10.1029/2012GL051574

McCutcheon, M.R., Staryk, C.J., Hu, X., 2019. Characteristics of the Carbonate System in a Semiarid Estuary that Experiences Summertime Hypoxia. Estuaries and Coasts. https://doi.org/10.1007/s12237-019-00588-0

Millero, F.J., 2010. Carbonate constant for estuarine waters. Mar. Freshw. Res. 61, 139–142.

Montagna, P. a, Brenner, J., Gibeaut, J., Morehead, S., 2011. Chapter 4: Coastal Impacts, in: Jurgen Schmandt, Gerald R. North, and J.C. (Ed.), The Impact of Global Warming on Texas. University of Texas Press, pp. 96–123.

R Core Team (2020). R: A language and environment for statistical computing. R Foundation for Statistical Computing, Vienna, Austria. URL https://www.R-project.org/.

Raymond, P. ~~a~~A., Cole, J.J., 2001. Gas e~~E~~xchange in r~~R~~ivers and e~~E~~stuaries: Choosing a g~~G~~as t~~T~~ransfer v~~V~~elocity. Estuaries 24, 312. https://doi.org/10.2307/1352954

Robbins, L.L., Lisle, J.T., 2018. Regional ~~A~~acidification t~~T~~rends in Florida s~~S~~hellfish e~~E~~stuaries: a 20+ Year l~~L~~ook at pH, o~~O~~xygen, t~~T~~emperature, and ~~S~~salinity. Estuaries and Coasts 41, 1268–1281. https://doi.org/10.1007/s12237-017-0353-8

Sastri, A.R., Christian, J.R., Achterberg, E.P., Atamanchuk, D., Buck, J.J.H., Bresnahan, P., Duke, P.J., Evans, W., Gonski, S.F., Johnson, B., Juniper, S.K., Mihaly, S., Miller, L.A., Morley, M., Murphy, D., Nakaoka, S.I., Ono, T., Parker, G., Simpson, K., Tsunoda, T., 2019. Perspectives on in situ ~~Sensors~~ sensors for ~~Ocean~~ ocean ~~Acidification~~ acidification ~~Research~~research. Front. Mar. Sci. 6, 1–6. https://doi.org/10.3389/fmars.2019.00653

Schulz, K.G., Riebesell, U., 2013. Diurnal changes in seawater carbonate chemistry speciation at increasing atmospheric carbon dioxide. Mar. Biol. 160, 1889–1899. https://doi.org/10.1007/s00227-012-1965-y

Seim, H.E., Kjerfve, B., Sneed, J.E., 1987. Tides of Mississippi Sound and the adjacent continental shelf. Estuar. Coast. Shelf Sci. 25, 143–156. https://doi.org/10.1016/0272-7714(87)90118-1

Semesi, I.S., Beer, S., Björk, M., 2009. Seagrass photosynthesis controls rates of calcification and photosynthesis of calcareous macroalgae in a tropical seagrass meadow. Mar. Ecol. Prog. Ser. 382, 41–47. https://doi.org/10.3354/meps07973

Solis, R.S., Powell, G.L., 1999. Hydrography, Mixing Characteristics, and Residence

Formatted: Indent: Left: 0", Hanging: 0.4", Widow/Orphan control, Adjust space between Latin and Asian text, Adjust space between Asian text and numbers, Pattern: Clear (White), Tab stops: 0.64", Left + 1.27", Left + 1.91", Left + 2.54", Left + 3.18", Left + 3.82", Left + 4.45", Left + 5.09", Left + 5.73", Left + 6.36", Left + 7", Left + 7.63", Left + 8.27", Left + 8.91", Left + 9.54", Left + 10.18", Left

Formatted: Font: Font color: Black, Check spelling and grammar, Border: : (No border)

Time of Gulf of Mexico Estuaries, in: Bianchi, T.S., Pennock, J.R., Twilley, R.R. (Eds.), Biogeochemistry of Gulf of Mexico Estuaries. John Wiley & Sons, Inc: New York, pp. 29–61.

Solis, R.S., Powell, G.L., 1999. Hydrography, Mixing Characteristics, and Residence Time of Gulf of Mexico Estuaries.

Takahashi, T., Sutherland, S.C., Sweeney, C., Poisson, A., Metzl, N., Tilbrook, B., Bates, N., Wanninkhof, R., Feely, R.A., Sabine, C., Olafsson, J., Nojiri, Y., 2002. Global sea-air CO2 flux based on climatological surface ocean pCO2, and seasonal biological and temperature effects. Deep. Res. Part II Top. Stud. Oceanogr. 49, 1601–1622. https://doi.org/10.1016/S0967-0645(02)00003-6

Thurman, H. V., 1994. Introductory Oceanography, seventh edition. pp. 252–276.

Uppström, L.R., 1974. The boron/chlorinity ratio of deep-sea water from the Pacific Ocean. Deep. Res. Oceanogr. Abstr. 21, 161–162. https://doi.org/10.1016/0011-7471(74)90074-6

USGS, 2001. Discharge Between San Antonio Bay and Aransas Bay, Southern Gulf Coast, Texas, May-September 1999.

Waldbusser, G.G., Salisbury, J.E., 2014. Ocean aAcidification in the cCoastal zZone from an oOrganism’s pPerspective: Multiple sSystem Pparameters, fFrequency dDomains, and hHabitats. Ann. Rev. Mar. Sci. 6, 221–247. https://doi.org/10.1146/annurev-marine-121211-172238

Wanninkhof, R., 1992. Relationship bBetween wWind sSpeed and gGas eExchange. J. Geophys. Res. 97, 7373–7382. https://doi.org/10.1029/92JC00188

Wanninkhof, R., Asher, W.E., Ho, D.T., Sweeney, C., McGillis, W.R., 2009. Advances in quantifying air-sea gas exchange and environmental forcing. Ann. Rev. Mar. Sci. 1, 213–244. https://doi.org/10.1146/annurev.marine.010908.163742

Weiss, R.F., 1974. Carbon dioxide in water and seawater: the solubility of a non-ideal gas. Mar. Chem. 2, 203–215.

Westfall, P.H., 1997. Multiple tTesting of gGeneral cContrasts Uusing lLogical cConstraints and cCorrelations. J. Am. Stat. Assoc. 92, 299–306. https://doi.org/10.1080/01621459.1997.10473627

Yao, H., Hu, X., 2017. Responses of carbonate system and CO_2 flux to extended drought and intense flooding in a semiarid subtropical estuary. Limnol. Oceanogr. 62, S112–S130. https://doi.org/10.1002/lno.10646

Yao, H., McCutcheon, M.R., Staryk, C.J., Hu, X., 2020. Hydrologic controls on CO_2 chemistry and flux in subtropical lagoonal estuaries of the northwestern Gulf of Mexico. Limnol. Oceanogr. 1–19. https://doi.org/10.1002/lno.11394

Yates, K.K., Dufore, C., Smiley, N., Jackson, C., Halley, R.B., 2007. Diurnal variation of oxygen and carbonate system parameters in Tampa Bay and Florida Bay. Mar. Chem. 104, 110–124. https://doi.org/10.1016/j.marchem.2006.12.008

Formatted: Subscript

Formatted: Subscript